國　立　交　通　大　學

電子工程學系電子研究所碩士班

碩　士　論　文

以電漿表面處理之新穎 REFET 製程

A novel fabrication of REFET with plasma surface treatments

學生：周庭暐　　Student : Ting-Wei Chou

指導教授：張國明 博士　　Advisor : Dr. Kow-Ming Chang

桂正楣 博士　　Dr. Cheng-May Kwei

中華民國九十五年六月

以電漿表面處理之新穎 REFET 製程

A novel fabrication of REFET with plasma surface treatments

學生：周庭暐　　Student : Ting-Wei Chou

指導教授：張國明 博士　　Advisor : Dr. Kow-Ming Chang

桂正楣 博士　　Dr. Cheng-May Kwei

國立交通大學電子工程學系電子研究所碩士班

碩士論文

A Thesis
Submitted to Department of Electronics Engineering & Institute of Electronics
College of Electrical Engineering and Computer Science
National Chiao Tung University
In Partial Fulfillment of the Requirements
for the Degree of
Master
In
Electronics Engineering
June 2006
Hsinchu, Taiwan, Republic of China

中華民國九十五年六月

以電漿表面處理之新穎 REFET 製程

學生:周庭暐　　　　　　　　　　指導教授:張國明 博士

桂正楣 博士

國立交通大學

電子工程學系 電子研究所碩士班

摘要:

Ion-sensitive field-effect-transistor（ISFET）最早是由 P.Bergveld 在 1970 年所提出的，其結構是將傳統的金氧半場效電晶體中的金屬閘極以待測溶液與參考電極所取代之。一旦待測溶液中的離子被感測層(sensing layer)表面的斷鍵所束縛住時，將會對下面的通道做出調變的效應，進而改變通道的電阻。如此一來，元件的電性將會隨著溶液的不同而產生變化，同時我們也可藉由電性的變化來判定溶液的性質。

而在應用上的問題則是來自於過多干擾,其中不乏光照射所產生的內部現象以及熱現象，於是相對應的元件則由此而生，而此元件設計的目的則在於抵銷光照效應以及熱效應,於是設計的原則則是與原 ISFET 具有一樣的光特性以及熱特性，但卻對 pH 的變化具有相對應低的感測能力，而此元件則稱之為 Reference field-effect-transistor(ReFET)，而在傳統的 REFET 設計，則是使用高分子有機化合物作為降低電場對通道的影響,而此在製程上的困難則是在於無法在同時間製作 ISFET/REFET，而必須有特殊製程針對 REFET 而設計，而在此研究中，我們則是以修補斷鍵作為製程設計的主要想法,進而採用電漿處理的方式進行斷鍵的修補，以使其具有低 pH 的感測能力並且可同時進行 ISFET/REFET 的製程。

A novel fabrication of REFET with plasma surface treatments

Student: Ting-Wei Chou

Advisor: Dr. Kow-Ming Chang

Dr. Cheng-May Kwei

Department of Electronics Engineering & Institute of Electronics

National Chiao Tung University

Abstract

The ion-sensitive field effect transistor (ISFET) was first introduced by P.Bergveld in 1970. The metal gate is replaced by a reference electrode and the electrolyte . Once the ions in electrolyte are trapped by the dangling bond at the surface of sensing layer , which will induce the modulation of channel resistance . Therefore, the electric characteristics are changed by different kinds of electrolyte , and we can distinguish the properties of electrolyte .

There are lots of interferences in application with ISFET. Such as lightening effect and thermal effect, to eliminate these effects and lower sensitivity of pH the Reference field-effect-transistor (REFET) were produced. The traditional REFET manufacturing is to gel macromolecular compounds reducing the modulation of channel by electric field. Then we need a special manufacturing process of REFET, and can not comanufacture ISFET/REFET. In this study, we use plasma to recover the dangling bonds from sensing layer. Then the comanufacturing process of ISFET/REFET pair is realized.

誌謝

兩年的時間很快的就在 NDL 裡面過去了，在電子所的這兩年中最要感謝的就是張國明老師每每的精神訓話，藉此激勵我持續研究的動力，以及桂正楣老師不厭其煩的教導我，使我能夠獲得新的靈感，沒有他們的照顧，我無法如此這麼順利的能夠完成學業，在這邊要感謝一位特別的老師，他是我以前的在中興物理時遇到的老師，。

此外要感謝的是趙高毅學長，在實驗的過程中他總是不厭其煩悉心教導我，使得我的實驗能夠進行順利，而也要感謝張知天學長對我的照顧以及提攜，特別在這邊要感謝知天學長指導我的論文寫作，我很幸運的遇到了兩位照顧學弟的博士班學長，而在這邊也要感謝兩位已經畢業的黃俊皓學長以及吳冠增學長，感謝他們指導我實驗的進行，以及教導儀器的使用。

同時也要感謝在 NDL 裡面所認識的人們，使得沉悶的實驗過程變得不在沉悶，無聊的等待時間變成有趣的休息時間，不熟悉的儀器變成熟悉，也要感謝實驗室裡溫暖的氣氛，特別是學長學弟們的鼓勵，使得我能夠獲得更多的動力能夠以進行我的研究。

最後，在這邊要感謝在我沉悶乏味的研究過程中一路陪伴我的女朋友，我想她才是我能夠堅持下去的最大動力，當然也感謝我的家人，有她們的支持，我才無後顧之憂，可以全心衝刺完成我的學業。

Content

Abstract (in Chinese)……………………………………………………………..i

Abstract (in English)……………………………………………………………..ii

Acknowledgements (in Chinese)…………………………………………………..iii

Contents……………………………………………………………………………iv

Figure captions……………………………………………………………….……vi

Table captions…………………………………………………………………….....ix

Chapter 1 Introduction

1.1 Motivation of this work…………..…………………………….……………1

1.2 Introduction to ISFET…………………………………..……………….……...1

1.3 Application of ISFET……………………………………..……………………3

1.4 Plasma treatment and REFET…………………………..………..………3

1.5 Thesis organization……………………………………………………………..4

1.6 References………………………………………………………………………4

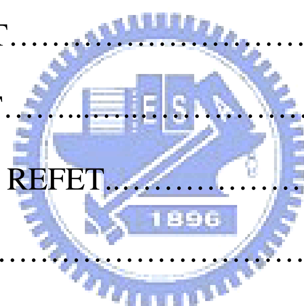

Chapter 2 Theory & Principle

2.1 Operation theory of ISFET………………………….................................8

2.2 The site-binding model and the sensitivity of ISFET……………………..…...11

2.3 The Principles of REFET………………………..………...……………..12

2.4 References…………………………………………………………………..17

Chapter 3 Experiment

3.1 Introduction……………..…………………………………………...…..18

3.2 Procedures of ISFET …..……………………………………………………..18

3.3 Experiment detail ……...………………..……………………………20

3.3.1 Gate region formation...………………..……………………………20

3.3.2 Sensing layer deposition……………………………………..……...21

3.3.3 Plasma treatment…………………………………..………………...21

3.3.4 S/D contact area deposition……………………………………………22

3.3.5 Device structure…………………………………………………...22

3.4 Measurement system……………………………………………….….23

3.4.1 Components affect the measurement…………………………………..23

3.4.2 Measurement setup……………………………………………………25

3.5 References……………………………………………………………..26

Chapter 4 Results and Discussions

4.1 Introduction……………………………………….……………………….…27

4.2 Sensitivity characteristic of sensing materials……………..………...…27

4.2.1 Sensitivity characteristic of TiO_2 membrane………………………….28

4.2.2 Sensitivity characteristic of ZrO_2 membrane…………………………29

4.3 The coplanar ISFET/REFET sensor array system………………...………30

4.3 Conclusions……………………………………………...……………30

Chapter 5 Future Work

5.1 Future work……………………………………………………………32

Figure Captions

Figure 1.1 The schematic of ISFET

Figure 2.1 ISFET structure band diagram

Figure 2.2 Potential profile and charge distribution at oxide / electrolyte interface

Figure 3.1 Experimental process

Figure 4.1 I-V curves of TiO2 without plasma treatment

Figure 4.2 Sensitivity chart of TiO2 without plasma treatment

Figure 4.3 I-V curves of TiO_2 membrane with NH_3 plasma treatment during 5 minutes

Figure 4.4 Sensitivity chart of TiO_2 with NH_3 plasma treatment during 5 minutes

Figure 4.5 I-V curves of TiO_2 membrane with NH_3 plasma treatment during 10 minutes

Figure 4.6 Sensitivity chart of TiO_2 with NH_3 plasma treatment during 10 minutes

Figure 4.7 I-V curves of TiO_2 membrane with NH_3 plasma treatment during 20 minutes

Figure 4.8 Sensitivity chart of TiO_2 with NH_3 plasma treatment during 20 minutes

Figure 4.9 I-V curves of TiO_2 membrane with NH_3 plasma treatment during 30 minutes

Figure 4.10 Sensitivity chart of TiO_2 with NH_3 plasma treatment during 30 minutes

Figure 4.11 I-V curves of TiO_2 membrane with NH_3 plasma treatment during 60 minutes

Figure 4.12 Sensitivity chart of TiO_2 with NH_3 plasma treatment during 60 minutes

Figure 4.13 The tendency of various plasma treating time interval of TiO_2

Figure 4.14 I-V curves of ZrO_2 without plasma treatment

Figure 4.15 Sensitivity chart of ZrO_2 without plasma treatment

Figure 4.16 I-V curves of ZrO2 membrane with NH3 plasma treatment during 5 minutes

Figure 4.17 Sensitivity chart of ZrO_2 with NH_3 plasma treatment during 5 minutes

Figure 4.18 I-V curves of ZrO_2 membrane with NH_3 plasma treatment during 10 minutes

Figure 4.19 Sensitivity chart of ZrO_2 with NH_3 plasma treatment during 10 minutes

Figure 4.20 I-V curves of ZrO_2 membrane with NH_3 plasma treatment during 20 minutes

Figure 4.21 Sensitivity chart of ZrO_2 with NH_3 plasma treatment during 20 minutes

Figure 4.22 I-V curves of ZrO_2 membrane with NH_3 plasma treatment during 30 minutes

Figure 4.23 Sensitivity chart of ZrO_2 with NH_3 plasma treatment during 30 minutes

Figure 4.24 I-V curves of ZrO_2 membrane with NH_3 plasma treatment during 60 minutes

Figure 4.25 Sensitivity chart of ZrO_2 with NH_3 plasma treatment during 60 minutes

Figure 4.26 The tendency of various plasma treating time intervals of ZrO_2

Figure 4.27 The coplanar structure

Table captions

Table 3.1 (a) Specifications of wafers

Table 3.1 (b) Parameters of sensing layers deposition with E – gun

Table 3.1 (c) Parameters of sensing layers deposition with Sputter

Table 3.1 (d) Condition of plasma treatment

Table 4.1 Sensitivity values of TiO2 with NH3 plasma treatment during time interval

Table 4.2 Sensitivity values of ZrO2 with NH3 plasma treatment during time interval

Table 4.3 The sensitivity of coplanar structure in TiO_2 membrane

Table 4.4 The sensitivity of coplanar structure in ZrO_2 membrane

Chapter 1

Introduction

1.1 Motivation of this work

All of the potentiometric sensors need a stable reference electrode to functionalize the sensor array system, the same condition as the Ion-sensitive field-effect-transistor (ISFET) system. In this work, the post plasma treatment was proposed to treat the sensing membrane surface. The sensing film deposited on gate oxide must be CMOS manufacturing compatible to achieve the cheap purpose. We choose TiO_2 and ZrO_2 as sensing films and the use of NH_3 plasma treats the surface of above films. The plasma treatment on sensing membrane surface is used to recover dangling bonds during short time surface treatment and become increasing dangling bonds during long time treatment, short/long time treatment is decided by what kinds of sensing membrane are. The influence on sensitivity will be presented in this work.

Furthermore, the coplanar structure of ISFET was used again. The purpose is to make a stable sensitivity on ISFET/REFET (reference field-effect-transistor) system in this work.

1.2 Introduction to ISFET

Because of the strong development of the IC technology on semiconductor, lots of applications of MOSFET are introduced. Such as the gas sensor, making the conductivity of the semiconductor in use [1], the pressure sensor , showing the variations of the capacitive on semiconductor [2], and the so called ISFET, exhibiting the variation of PH value by the electrical characteristic of FET.

All that we know the operation mode of MOSFET, and the same operation mode of ISFET, unless take the reference electrode and the PH solution (or electrolyte solution) replace the metal gate. The gate material of ISFET, as the same part called gate dielectric of the MOSFET, called sensing layer, immersed in the electrolyte solution, as shown in Fig. 1.1.

The first thought to detect variations of the ion concentration by using FET was introduced by P. Bergveld , in 1970 [3]. The most of the advantages of ISFET are small size making multiple sensors on a chip, fast response, mass producible, and cheap cost possibility. And the manufacturing process is similar to the MOSFET. The same behavior to MOSFET, the channel resistance in ISFET depends on the electric field perpendicular to the direction of the drain current. The different pH solution makes the different concentration of H^+-ion. The H^+-ions from the electrolyte accumulate on the top of the sensing material, and do hardly permeating through the ion-sensing membrane. Such reaction described above causes the potential drop on the sensing membrane surface.

The phenomenon of the different H^+-ion concentration forming the different channel resistance can be explained by the well known site-binding model, introduced by Yates et al [4], in 1974. This model is different from the porous gel model suggested by Lyklema [5], having the very high values of titratable charge on some oxides. In this model, introduced by Yates et al, the oxide surfaces was considered as amphoteric, meaning that the surface hydroxyl groups can be natural , protonized (positively charged) or deprotonized (negatively charged) depending on the pH of the electrolyte. Furthermore, T. Hiemstra et al [6] introduced the MUSIC model to explain the other physical parameter influence the binding condition, such as the orientation of sensing membrane surface etc. An general model to describe the sensitivity of ISFET was introduced by van Hal et al [7], thus, the theory of ISFET

was developed well.

1.3 Applications of ISFET

Because of the well development theory of EOS structure, and the detection methods become more mature, more and more applications of ISFET were developed. Such as EnFET [8], it is same as ISFET replace the sensing membrane as enzyme stacking upon the pH-sensitive membrane reacting with the specific matter in the buffer solution. Environmental monitor with the pH value of soil uses the pH-ISFET, because of pH-ISFET's fast responds, by inserting into the soil in situ without digging the soil and taking it into laboratory to analyze [9]. Even for detecting the diffusion coefficient of the solution [10]. Furthermore, biochemical usage is to embedding the specific chain of DNA such as ACTACTA on the sensing layer surface, the other DNA chain such as TGATGAT in the solution, when the sensing layer immersed in the solution the DNA was coupled and potential drop appearance [11]. However, all the potentiometric sensor array needs a reference field effect transistor to calibrate sensitivity in the system. Most of manufacturing REFET covers the PVC membrane or plastic material onto sensing membrane to insense with electrolyte. Thus, we can not fabricate ISFET/REFET sensor array at the same time to reduce the cost. In this work, in the point of view of theory the purpose is to make co-manufacturing process of ISFET/REFET sensor array.

1.4 Plasma treatment and REFET

Thus, knowing from the above described, the sensing properties of pH-ISFET are

depending on various materials and the situation of oxide/electrolyte interface. Whatever the materials covered on the gate layer are, the main purpose of using the PVC membrane or Nifon is to reduce the influence of channel region and suppress ion interfering effects[12][13]. Here, the purposed plasma treatment method is finding other way to do so, and it's also reducing the complex process to glue the PVC membrane or Nifon on the gate. And membranes ZrO_2 and TiO_2 are used in this work, because of the stable electrical characteristic compared to the Si_3N_4 [14] , and SiO_2 [14]. And the higher sensitivity then Si_3N_4 and SiO_2 [15] films will be presented in this work.

According to the theory of site-binding model, the sensitivity of pH-ISFET is related to the influence of interface between oxide and electrolyte. The plasma treatment is proposed for trying to recover the dangling bonds in this work to reduce sensitivity. The manner of plasma treatment is usually breaking the bond between the atoms, making more dangling bonds on the sensing membrane surface during longer time treatment and recovering dangling bonds during shorter time treatment. Here, the combination between plasma radicals and surface atoms for shorter treating time presents lower sensitivity than without plasma treatment, and the higher sensitivity for longer treating time. Whatever, a result of either making more trap state (dangling bond) of H^+-ions or combination between plasma radicals and surface atoms (recover dangling bonds) can be seen from the relationship between sensitivity and surface plasma treating time by TiO_2 sensing membrane with NH_3 plasma treatment. In this work, we are trying to find the best process windows for TiO_2 and ZrO_2 sensing membranes

Finally, the coplanar structure can form a coupled ISFETs or just a REFET by the difference which eliminates the unnecessary interferences such as temperature effects, ion perturbations and lightening conditions under detection.

1.4 Thesis organization

In the first chapter, a brief history of ISFET and the theory developed by those great people was introduced. And the reason why we use plasma to treat the sensing membrane surface is also addressed in chapter 1. The detailed theory, including the band diagram of ISFET, site-binding model introduced by Yates et al , and the sensitivity of ISFET, are described in chapter 2. In this chapter, the brief introduce of REFET is presented. In the next section, the entire experiment procedures and measurement setup is presented in detail. The various kinds of sensing membrane are used to produce the coplanar structure ISFET-REFET pairs. In the last two chapters, some thoughts about the results are proposed and the conclusions are presented, too. Finally, some works are presented to do in the future.

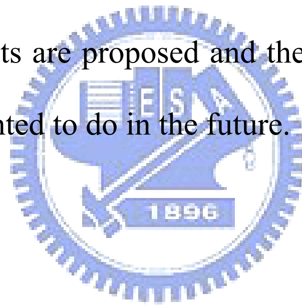

1.5 References

[1] Yong Jiang, Wulin Song, Changsheng Xie, Aihua Wang, Dawen Zeng, Mulin Hu, "Electrical conductivity and gas sensitivity to VOCs of V-doped ZnFe2O4 nanoparticles" , Material Letters, 60(2006) p.1374-1378

[2] M. Zagnonia, A. Golfarelli, S. Callegari, A. Talamelli,V. Bonora, E. Sangiorgi, M. Tartagni, "A non-invasive capacitive sensor strip for aerodynamic pressure measurement" , Sensors and Actuators: A. Physical 123-124 complete(2005) p240-248

[3] P. Bergveld , "Development of an ion sensitive solid-state device for neurophysiological measurements" , IEEE Trans.Biomed. Eng.,vol. BME-17 (1970) p.70

[4] D.E. Yates , S. Levine and T.W. Healy , "Site-binding model of the electrical

double layer at the oxide/wafer interface ” , J. Chem. Soc. Faraday Trans. , 70 (1974) p.1807-1818

[5] J. Lyklema, “The electrical double layer on oxides” , Croatica Chem. Acta, 43 (1971) p.249

[6] T. Hiemstra, W. H. van Riemsdijk, and G. H. Bolt, “Multisite Proton Adsorption Modeling at the Solid/Solution Interface of (Hydr)oxides: A New Approach” , J. Colloid and Interface Sci. 133(1989) p91

[7] R. E. G. van Hal, J. C. T. Eijkel, P. Bergveld, “A general model to describe the electrostatic potential at electrolyte oxide interfaces” , Colloid interface Sci. 68(1996) p.31-62

[8] Alexey P. Soldatkin et al, “Analysis of the potato glycoalkaloids by using of enzyme biosensor based on pH-ISFETs” , Talanta 66(2005) p.28-33

[9] Henning Matthiesen, “In situ measurement of soil pH” , J. of Arch. Sci. 31(2004)p.1373-1381

[10] Arshak Poghossian et al, “Chemical sensor as physical sensor: ISFET-based flow-velocity,flow-direction and diffusion-coefficient sensor” , Sensors and Actuators B 95(2003) p.384-390

[11] P. Estrela et al, “Field effect detection of biomolecular interactions” , Electrochimica Acta 50 (2005) p.4995-5000

[12] Z.M. Baccar, N. Jaffrezic-Renault , C. Martelet , H. Jaffrezic, G. Marest, A. Plantier
“Sodium microsensors based on ISFET/REFET prepared through an ionimplantationprocess fully compatible with a standard silicon technology”
Sensors and Actuators B 32 (1996) 101-105

[13] Michal Chudy, Wojciech Wro´ blewski, Zbigniew Brzo´zka "Towards REFET" Sensors and Actuators B 57 (1999) 47–50

[14]Fukuzawa Y, "Machining characteristics of insulating ceramics by electrical discharge machine" INDUSTRIAL CERAMICS 21 (3): 187-189 SEP-DEC 2001

[15]Jung-Chuan Chou, "Sensitivity and hysteresis effect in Al2O3 gate pH-ISFET" Materials chemistry and physics 71(2001) 120-124

Chapter 2

Theory & Principle

2.1 Operation theory of ISFET

The operation theory of an Ion Selective Field Effective Transistor (ISFET) is similar to a MOSFET. Considering the following structure of a MOSFET

Al_b | Si | SiO2 | Al_t

Al_b : the back side of silicon coated Al as electrode

Al_t : the top side of silicon coated Al as S/D/G electrical contact

Before the different materials contact to each other, the flat-band voltage is build. [1] When these materials contact to each other and form a MOSFET structure, which result in the potential differences in between these materials has been presented in the band diagram. Through the band diagram, we can obtain the flat band voltage as the E.q.

$$V_{FB} = \frac{1}{q}\Phi_{ms} - \frac{Q_{SS}}{C_{OX}}$$

The same properties of ISFET are presented as following. The electrolyte layer was inserted in between oxide and metal layer, and we take the SiO2 film as the sensing layer to detect the specific ions in electrolyte. Forming the following structure,[2]

$$Al_b\ |^1\ Si\ |^2\ SiO2\ |^3\ Electrolyte\ |^4\ M\ |^5\ Al_t$$

The couple layer M | Al_t was taken as the reference electrode. The reference electrode is not the key subject in this study, the considered couple layer presented here is used to simplify the model of reference electrode. Figure 2.1 shows the above ISFET structure band diagram. Considering the above structure as cell, then the applied voltage of the cell can be written as follows

$$V_a = \phi^{Al_t} - \phi^{Al_b} = -\frac{1}{q}\overline{\Phi}^{Al_t} + \frac{1}{q}\overline{\Phi}^{Al_b} \tag{1}$$

Due to the equilibrium at interfaces 1 and 5 , Eq.(1) reduced to

$$V_a = -\frac{1}{q}\overline{\Phi}^{M} + \frac{1}{q}\overline{\Phi}^{Si} = -\frac{1}{q}\Phi^{M} + \frac{1}{q}\Phi^{Si} + (\phi^{M} - \phi^{Si}) \tag{2}$$

Where the electrochemical potentials have been considered as chemical and electrical contributions. Because of the electrical contributions, the reference electrode part must be considered. The following Eq. is the definition of reference electrode.

$$E_{ref} = -\frac{1}{q}\Phi^{M} + (\phi^{M} - \phi^{Si}) \tag{3}$$

Here E_{ref} was named “reduced absolute electrode potential” by Trasatti[R].

Substituting the Eq.(3) into Eq(2) gives

$$V_a = E_{ref} + \frac{1}{q}\Phi^{Si} + \phi^{Sol} - \phi^{Si} \tag{4}$$

The difference terms solution bulk (φ^{sol}) and silicon bulk(φ^{Si}) , can be separated as follows

$$\phi^{Sol} - \phi^{Si} = (\phi_b^{Sol} - \phi_d^{Sol}) + (\phi_d^{Sol} - \phi_d^{OX}) + (\phi_d^{OX} - \phi_0^{OX}) + (\phi_0^{OX} - \phi_0^{Si}) + (\phi_0^{Si} - \phi_b^{Si}) \tag{5}$$

As can be seen in band diagram (Fig2.1), each term on the right hand side can be interpreted

$$\phi_b^{Sol} - \phi_d^{Sol} = -\psi_0 \tag{6}$$

Where ψ_0 is the potential drop in the electrolyte at the oxide/electrolyte interface

$$\phi_d^{OX} - \phi_0^{OX} = V_{OX} \tag{7}$$

$$\phi_0^{Si} - \phi_b^{Si} = \psi_S \tag{8}$$

The potential drop across the oxides (V_{ox}) and the silicon surface potential (ψ_0) are presented above

$$\phi_d^{Sol} - \phi_d^{OX} = \delta_{OX}^{Sol}(dipole) = (\mathrm{X}^{Sol} + \delta\mathrm{X}_{OX}^{Sol}) - (\mathrm{X}^{OX} + \delta\mathrm{X}_{Sol}^{OX}) \tag{9}$$

$$\phi_0^{OX} - \phi_0^{Si} = (\mathrm{X}^{OX} + \delta\mathrm{X}_{Si}^{OX}) - (\mathrm{X}^{Si} + \delta\mathrm{X}_{OX}^{Si}) \tag{10}$$

From Eqs (4)-(8) and (9) and (10) the following expression for the flat-band voltage is obtained as below

$$V_{FB} = E_{ref} - \psi_0 - \frac{1}{q}\Phi^{Si} + \mathrm{X}^{Sol} + (\delta\mathrm{X}_{OX}^{Sol} - \delta\mathrm{X}_{Sol}^{OX}) + (\delta\mathrm{X}_{Si}^{OX} - \delta\mathrm{X}_{OX}^{Si}) - \frac{Q_{SS}}{C_{OX}} \tag{11}$$

Taking the perfect interface of oxide/solution and oxide/silicon into account, meaning that the condition of interface is not concluded in this study, the following Eq. is obtained

$$(\delta\mathrm{X}_{OX}^{Sol} - \delta\mathrm{X}_{Sol}^{OX}) + (\delta\mathrm{X}_{Si}^{OX} - \delta\mathrm{X}_{OX}^{Si}) = 0 \tag{12}$$

Thus, the flat-band voltage, suited with the EOS structure, is obtained

$$V_{FB} = E_{ref} - \psi_0 - \frac{1}{q}\Phi^{Si} + \mathrm{X}^{Sol} - \frac{Q_{SS}}{C_{OX}} \tag{13}$$

The ψ_0 term, which is presented in Eq(13), determines the operation of the EOS structure as chemical sensor. It depends mainly on the solution pH, in the case of oxide material???. In particular, the solution pH at which ψ_0 = 0 is called the pH_{pzc} (point of the zero charge)

2.2 The site-binding model and the sensitivity of ISFET

According to the above detail, the parameter of ψ_0 plays an important role of the sensitivity. Obviously, the interface condition on oxide/solution must be considered by the combination of the oxide-ion. Yates et al [3] introduced the site-binding model based on the adsorbed counter ion form interfacial ion pairs with discrete charged surface groups. The direction of plane was considered [4], but did not make the same consideration in this study. And the influence of the porosity of the layer [5] was not concluded here.

Considering the oxide surfaces as amphoteric, meaning that the surface hydroxyl groups can be natural, whatever positively charged (protonized) and negatively charged (deprotonized). The charging mechanism of an oxide is the result of equilibrium between the AOH surface sites and the H^+-ions in the bulk of the solution. And the surface dissociation reactions are [6] :

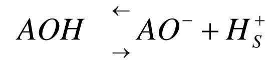

$$AOH \underset{\rightarrow}{\overset{\leftarrow}{}} AO^- + H_S^+$$

and

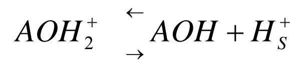

$$AOH_2^+ \underset{\rightarrow}{\overset{\leftarrow}{}} AOH + H_S^+$$

where s means the surface

From above reaction we can get the following thermodynamic equations :

$$\mu_{AOH}^0 + kT \ln \nu_{AOH} = \mu_{AO^-}^0 + kT \ln \nu_{AO^-} + \mu_{H_S^+}^0 + kT \ln a_{H_S^+} \tag{1}$$

and

$$\mu_{AOH_2^+}^0 + kT \ln \nu_{AOH_2^+} = \mu_{AOH}^0 + kT \ln \nu_{AOH} + \mu_{H_S^+}^0 + kT \ln a_{H_S^+} \tag{2}$$

where ν_i is the surface activity and μ^o_i is the standard chemical potential of species i.

Following Eq. (1) and (2) and the definition of the activity between surface and

bulk solution

$$a_{H_S^+} = a_{H_S^+} \exp\frac{-q\psi_0}{kT} \tag{3}$$

we have Eq. (3) and (4) as below

$$\frac{\nu_{AOH^-} a_{H_S^+}}{\nu_{AOH}} = K_a \qquad \text{with} \qquad K_a = \exp\frac{\mu^0_{AOH} - \mu^0_{AO^-} - \mu^0_{H_b^+}}{kT} \tag{4}$$

$$\frac{\nu_{AOH} a_{H_S^+}}{\nu_{AOH_2^+}} = K_b \qquad \text{with} \qquad K_b = \exp\frac{\mu^0_{AOH_2^+} - \mu^0_{AOH} - \mu^0_{H_b^+}}{kT} \tag{5}$$

where the K values are dimension less intrinsic dissociation constants. From the above Eqs , showing that the K values are real constants independent of the ionization state of the oxide surface. Then the surface charge density, ν_i , is obtained as follows

$$\sigma_0 = q(\nu_{AOH_2^+} - \nu_{AO^-}) = qN_s(\Theta^+ - \Theta^-) \tag{6}$$

where Ns is the density of the available sites; Θ^+ and Θ^- are the fractions AOH_2^+ and AO^- of Ns, respectively. The fractions Θ^+ and Θ^- can be calculated by Eqs (1) and (2) as follows

$$\sigma_0 = qN_s\left(\frac{a^2_{H_S^+} - K_a K_b}{K_a K_b + K_b a_{H_S^+} + a^2_{H_S^+}}\right) = -q[B] \tag{7}$$

Taking the pH variations in the oxide/electrolyte interface into account, then the surface charge density versus the pH variation on the surface can be calculated as following definition

$$\frac{\delta\sigma_0}{\delta pH_S} = -q\frac{\delta[B]}{\delta pH_S} = -q\beta_{\text{int}} \tag{8}$$

β_{int} is called intrinsic buffer capacity, depending on the activity of surface H^+-ions .

And thus we can finally find the expression for the intrinsic buffer capacity

$$\beta_{\text{int}} = N_S \frac{K_b a_{H_S^+}^2 + 4K_a K_b a_{H_S^+} + K_a K_b^2}{(K_a K_b + K_b a_{H_S^+} + a_{H_S^+}^2)^2} 2.3 a_{H_S^+} \tag{9}$$

Because of the β_{int} is dependent on the variation of surface charge density and activity of surface H^+-ions, we may consider the intrinsic buffer capacity as the parameter for the sensing material. And that , there are several parameters affecting the active surface groups, e.g. the valence of the metal ion. Hiemstra et al.[7] introduced a multisite complexation model (MUSIC) to describe the charging mechanism and to estimate the value of intrinsic dissociation constants of the active surface groups from physical parameters. But these factors are specific for any particular oxides having different reactive groups are present on different oxides. The general expression for all types of oxides can not be achieved. Every oxide should be treated separately. Because of the amorphous type of the sensing layer on the ISFET in this experiment, the MUSIC model is not suitable here.

Next, according to the charge neutrality, an equal but opposite charge is built up, σ_{DL}, in the electrolyte solution side of the double layer. Thus there will be, something like capacitor (Fig2.2), built up in the oxide/electrolyte system. We can obtain the following Eq. by such equilibrium in Boltzmann equation:

$$c_i(x) = c_i^0 \exp\left(\frac{-z_i q \phi_x}{kT}\right) \tag{10}$$

Where φ_x is the potential at any distance x with respect to the bulk of the solution; $c_i(x)$ and c_i^0 are the molar concentrations of species i at a distance x and in the bulk of the solution respectively and z_i is the magnitude of the charge on the ions. And the combination of the Boltzmann and Poisson equation the related charge density with the potential is obtained as follows:

$$\sigma_{DL} = -(8kT\varepsilon\varepsilon_0 n^0)^{\frac{1}{2}} \sinh\left(\frac{zq\phi_2}{2kT}\right) = -C_0\psi_0 = -\sigma_0 \tag{11}$$

Considering that the ions adsorbed on the oxide/electrolyte interface as a couple layer ,

inner layer (Stern layer) and outer layer (diffuse layer) , made the potential drop on the distance x_2.

Thus Eq (12) is considered,

$$\phi_2 = \psi_0 - \frac{\sigma_0 x_2}{\varepsilon\varepsilon_0} \tag{12}$$

Instead Eq(12) in Eq(11) , and differentiating and rearranging Eq(11) , gives the following equation :

$$C_{dif} = \frac{\left(\frac{2\varepsilon\varepsilon_0 z^2 q^2 n^0}{kT}\right)^{\frac{1}{2}} \cosh\left(\frac{zq\phi_2}{2kT}\right)}{1 + \left(\frac{x_2}{\varepsilon\varepsilon_0}\right)\left(\frac{2\varepsilon\varepsilon_0 z^2 q^2 n^0}{kT}\right)^{\frac{1}{2}} \cosh\left(\frac{zq\phi_2}{2kT}\right)} \tag{13}$$

To simplify the above equation as follows

$$\frac{1}{C_{dif}} = \frac{x_2}{\varepsilon\varepsilon_0} + \frac{1}{\left(\frac{2\varepsilon\varepsilon_0 z^2 q^2 n^0}{kT}\right)^{\frac{1}{2}} \cosh\left(\frac{zq\phi_2}{2kT}\right)} \tag{14}$$

There will be seen easily , the differential capacitance can be distinguish into two parts , the first term is the contribution of the called Stern layer , the second term is the contribution of the diffuse layer. Then the following equation will be obtained:

$$\psi_0 = \frac{\sigma_0}{C_{i,d}} + \frac{\sigma_0}{C_{i,st}} = \phi_2 + \frac{(8kT\varepsilon\varepsilon_0 n^0)^{\frac{1}{2}} \sinh\left(\frac{zq\phi_2}{2kT}\right)}{C_{i,st}} \tag{15}$$

From now, the appearance of sensitivity will be discovered. Considering the activity between surface and bulk solution , the Eq(3) is repeated here.

$$a_{H_S^+} = a_{H_B^+} \exp\frac{-q\psi_0}{kT} \tag{16}$$

From above equation, we can obtain the following expression ,

$$pH_S = pH_B + \frac{q\psi_0}{2.3kT} \tag{17}$$

Taking the surface charge density into account , the variation of σ_0 versus the potential drop will be presented as follows,

$$\frac{\delta\sigma_{DL}}{\delta\psi_0} = -\frac{\delta\sigma_0}{\delta\psi_0} = C_{dif} \tag{18}$$

Combination of (8) and (18) leads to an expression for the sensitivity of the electrostatic potential towards changes in $a_{H_S^+}$:

$$\frac{\delta\psi_0}{\delta pH_S} = \frac{\delta\psi_0}{\delta\sigma_0}\frac{\delta\sigma_0}{\delta pH_S} = -\frac{q\beta_{\text{int}}}{C_{dif}} \tag{19}$$

The next expression is given by the combination of (19) and (17)

$$\frac{\delta\psi_0}{\delta(pH_B + \frac{q\psi_0}{2.3kT})} = -\frac{q\beta_{\text{int}}}{C_{dif}} \tag{20}$$

Finally, rearranging of (20) gives a general expression for the sensitivity of the electrostatic potential to changes in the bulk pH:

$$\frac{\delta\psi_0}{\delta pH_B} = -2.3\frac{kT}{q}\alpha \tag{21}$$

Where

$$\alpha = \frac{1}{\frac{2.3kTC_{dif}}{q^2\beta_{\text{int}}} + 1} \tag{22}$$

The sensitivity parameter α is dimensionless and the value varies between 0 and 1 depending on the intrinsic buffer capacity and the differential capacitance. Where the maximum value of sensitivity is about 60 mV/pH. In the experiment of this study, the higher sensitivity about 70 mV/pH is presented, however , the theory of the higher value of sensitivity are still discussing. Does the lower sensitivity of the ISFETs be useless ? According to the introduction of REFET , the principle of REFET will be presented as the following section.

2.3 The Principles of REFET

Because the requirements of a stable reference electrode for the potentiometric sensors to do proper functioning, the same meaning as the ISFET , the so called reference field effect transistor (REFET) is developed. The major characteristic of REFETs is the lowest sensitivity for the detection under such an environment we appointed. A pH REFET is developed in such a thought, making the lower sensitivity of pH. Considering the theory of ISFET is described above, the sensitivity parameter α relates the differential capacitance and the intrinsic buffer capacity , as pointed to Eq(22).

From the eq(22) where the lower sensitivity appeared , the lower intrinsic buffer capacity will also be obtained. The issue of intrinsic buffer capacity and it's relation to the effective sites (N_S) on the interface between oxide/electrolyte is described and is observed in the eq(8). An assumption of the lower sensitivity was proposed by recover the effective sites (N_S) on the interface between oxide/electrolyte. Plasma treatment is one of solutions proposed to recover the dangling bonds on the interface between oxide/electrolyte. As can be seen in the final result of the experiment, the sensitivity was reduced successfully by such post plasma treatment on the sensing material surface.

In the experiment, we will discuss the effects of the plasma treatment. Which include the nitridation of NH_3 plasma and the increase of the site density of dangling bonds on the sensing membrane surface.

2.4 References

1. Neamen, Donald A , “Semiconductor physics and devices :basic principles”, McGraw-Hill , 2003

2. Luc Bousse , “Single electrode potentials related to flat-band voltage measurements on EOS and MOS structures” J. Chem. Phys. , 76 , (1982) p.5128-p.5133

3. D.E. Yates , S. Levine and T.W. Healy ,“ Site-binding model of the electrical double layer at the oxide/wafer interface ”, J. Chem. Soc. Faraday Trans. , 70 (1974) p.1807-1818

4. Fabien Gaboriaud , and Jean-Jacques Ehrhardt , “Effect of different crystal faces on the surface charge of colloidal goethite (α-FeOOH) particles: An experimental and modeling study” , Geochimica et Cosmochimica Acta, 67(2003) p. 967-983

5. J. Lyklema , “The electrical double layer on oxides” , Croatica Chem. Acta, 43 (1971) p249

6. R. E. G. van Hal, J. C. T. Eijkel, and P. Berveld , “A general model to describe the electrostatic potential at electrolyte oxide interfaces” , Adv. Colloid Interface Sci. 68 (1996) p.31-62

7. T. Hiemstra, J. C. M. de Wit, and W. H. van Riemsdijk, “Multisite proton adsorption modeling at the Solid/Solution interface of (Hydr) oxides: A New Approach II. Application to various important (Hydr)oxides”, J. Colloid and Interface Sci. , 133(1989) p. 105-116

Chapter 3

Experiment

3.1 Introduction

ISFET has the same manufacturing process as the conventional MOSFET. The difference in MOSFET and ISFET procedure is the process of gate electrode. The ISFET take the gate membrane as a sensing layer immersed in the pH-solution [1], and the reference electrode is placed overhead the sensing layer as the gate voltage controller. Furthermore, the strong development of IC industry assists the procedure of ISFET more easily, but there still have a lot of problems confused us. Purposed plasma treatment on sensing layer may find a way out of the confused issue. Furthermore, applying the successful integration-circuit technology, the ISFET devices have potential advantages over conventional ion selective glass electrodes in their rapid response, low cost, small size, high input impedance and low output impedance.

3.2 Procedures of ISFET

All procedures of experiment are done in NDL (National Nano Device Laboratory) and NFC (Nano Facility center), similar to the manufacturing process of MOSFET [2]. The corresponding diagram of ISFET is shown in Figure 3.1. The sensing layers titanium dioxide and zirconium dioxide are deposited onto the SiO_2 gate ISFET which prepared by E-gun and Sputter in Nano Facility center. Before every step, besides after sensing membrane deposited onto SiO_2 gate, the initial clean immersed in

H_2SO_4+H_2O_2 about 5 minutes and dipped in HF solution were done. The fabrication parameters are listed in Table 3.1, and the fabrication procedures are listed as follows:

1. RCA clean .
2. Wet oxidation 6000 Å .

    Temperature = 1050℃ for 65 min .
3. Mask - Ⅰ. S / D definition .
4. BOE etch wet oxide .
5. Dry oxidation for screening 300 Å .

    Temperature = 1050℃ for 12 min .
6. S / D implantation .

    5e15 ($1/cm^2$)，25Kev (Phosphorus)

7. N-type annealing .

    Temperature = 950℃ for 30 min .
8. PECVD - oxide for 1 μm .
9. Mask - Ⅱ. contact hole & gate region definition .
10. BOE etch PECVD - oxide for 1 μm (contact hole region) .

    PECVD - oxide for 1 μm+ wet oxide for 6000 Å (gate region) .
11. Dry oxidation 100 Å (gate oxide) .

    Temperature = 850℃ for 60 min .
12. Sensing layer deposition .

    * *Deposit titanium dioxide by E-gun and zirconium dioxide by sputter, respectively*
13. Plasma treatment

    **We use the NH_3 plasma to treat the sensing membrane surface by*

several time interval.

14. Annealing in pure O_2 .

Temperature = 850℃ for 60 min .

15.Thermal coating of Al (electrical contact) 5000 Å .

16.Sintering Al electrode

Temperature = 400℃ for 30 min .

3.3 Experiment detail

3.3.1 Gate region formation

At the beginning, The RCA clean has to be done. RCA clean was used to reduce possible pollution such as particles, organics, diffusion ions and native oxide. For the good performance in this work, we take the RCA clean carefully. And for a good efficiency, the p-type wafers were purchased from CARTINA. The device structure was definite before wet oxidation. Following above step, the SiO_2 was grown by thermal wet oxidation 600nm for blocking layer under the S/D ion implantation. The density and the energy of S/D implant is 5E15 ($1/cm^2$) and 25Kev with phosphorus dopant, respectively. After S/D implantation, following a 950℃ 30 minutes N+ anneal in N_2 gas performed to activate the dpants. Noted that, in the following experiment, the temperature here, must be lower than the annealing temperature to prevent dopant redistribution.

After all, the PE-oxide film about 1 μm was deposited onto the original 600nm thickness oxide, which protect the structure of a pH-ISFET blocking the ions diffuse when immersed in electrolyte. Thus, a stable electrical characteristic can be obtained. Next, the gate region was definite by lithography. Before deposit sensing membrane,

the 100A think oxide grown in oven as gate oxide, making the sensing layer adhesion more tightly.

3.3.2 Sensing layer deposition

Methods of deposited sensing membrane as gate material are different. And the deposition methods decide the electrical characteristic of pH-ISFET affected by the inner cave [3]. Before this work, the research about method of deposit sensing membrane has been done by the group I belong to. Thus, in this work, titanium dioxide is prepared by E-gun under the degree of vacuity about 10^{-6} and zirconium dioxide are deposited by sputter to reduce the inner cave under the degree of pressure about 10^{-3} (here, the sputter is pumped till the degree of pressure about 10^{-6} first, then the argon plasma is used to sputter the target material). To prevent the sensing membrane react with acid/base, the hard mask is used in such a thought. The detailed parameters of sputter are listed in Table 3.1 (c). Table 3.1 (b) lists the parameters of the dual E-gun system.

3.3.3 Plasma treatment

Subsequently, the PECVD system is used to produce plasma to treat the sensing layer. The plasma system used in this work, located in the Nano Facility center in National Chiao-Tung University, Hsinchu. Three kinds of plasma are used to do such a treatment in the first round of the experiment. The NH_3 plasma is used to treat sensing membrane surface for several time interval. The PECVD system is a couple of parallel planes which is DC-biased. The one is that RF power increases, it will make a greater dissociation rate of gas molecules and it induces more reactive species

in plasma for the higher RF input power. The RF power determinates the plasma density, thus we generate the power towards 100 watts. The inner chamber pressure is set to be 200mtorr, where the chamber pressure limits the quantity of total reactant gases existed in the chamber. The gas flow rate is set to be 30 sccm, trying to control the situation into stable under plasma treatment. Finally, we can see the fluorescent emission from the window near the substrate surface in the chamber. Table 3.5 lists the parameters when do such a treatment.

3.3.4 S/D contact area deposition

The process of the ISFET is still going on, in the next step we put the post plasma treatment wafer into an oven to anneal. The purpose of sensing layer annealing is to make the combination between SiO_2 and sensing membrane tightly. To prevent the sensing layer come into crystal, the temperature is set about 600℃, whatever which one kind of sensing layer.

Following sensing layer annealing, the source/drain contact was deposit onto the substrate. The hard mask is used again in this step to definite the S/D contact area. In deposition of S/D contact area, thermal coating of Al is deposited on the wafer topside for S/D electrical contact area and it's thickness is about 5000A Deposition on backside for back electrical contact by Al film and the thickness is about 5000A. The method of deposition backside is thermal coating. Thus the next step, sintering is to make the contact into ohmic contact to reduce the contact resistance.

3.3.5 Device structure

Considering the manufacturing of MOSFET, the coplanar structure was purposed. Thus, the ISFET-REFET made in the same time. The REFET, we described above, gate material usually made by PVC membrane to decrease the affect by the potential drop under different electrolyte, furthermore, Teflon was the material in used too. However, such a manufacturing can not apply in the CMOS procedure, an extra manufacturing for REFET is necessary. Furthermore, the coplanar structure can minimize the ion interference by difference and eliminate the inaccuracy during the manufacturing process of ISFET-REFET. Eventually, the characteristic behavior by minus the coplanar structure can produce a single ISFET. The device size here is large to avoid the short channel effects and decrease the other interferences in the semiconductor [4].

3.4 Measurement system

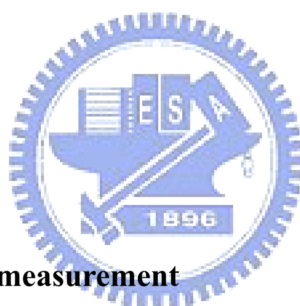

3.4.1 Components affect the measurement

Considering the interferences of the measurement, the sources of errors in chemical sensors was discussed as following. For obtain more precise measurement results, the errors was separated by chemical, instrumental and non-chemical [5] , and discussed as follows,

Sources of errors of chemical causes includes:

Ion interferences – exceed one above analytical signals will interfere to each other cause an ideal chemical sensor can’t exhibit the changes in the analytical signal caused only by the analyte. In our measurement, the ion interferences happened when change solution from acid to base or vise verse, therefore, detailed dilution is essential to reduce ion interferences.

Calibration procedure – some problems are response time of the sensor and its hysteresis. During the calibration process a concentration gradient develops, which influence on diffusion of the analyte through the chemical interface of the sensor until the equilibrium state is achieved. Usually, the diffusion process is quite slow being mainly determined by the thickness of the chemical interface. One proper solution is to wait until a steady state is reached.

Leakage of the chemical interface components – the membrane of ISFET is fabricated by difference conditions so that interface characteristics differ. One problem is that chemical interface component will be leaked out to the sample. In the case of potentiometric sensors, like ISFET, usually the ionophere is physically entrapped inside the membrane. The leakage of the membrane components leads to drift in the sensor signal and result in limited lifetime of the sensor if leakage continuous.

Liquid junction potential – the composition of the electrolyte to be measured can differ from the solutions used in the calibration process, the slope of the calibration curve varies slightly, this phenomenon caused by the uncertainty in the liquid junction potential. No matter how precise a sensitive equipment is used, this error cannot be eliminated or compensated. The literature data [6] indicate that the minimal relative error in the measured activity is about +/- 4% for univalent ion.

Sample composition – due to unknown and unpredictable compositions of sample used in laboratory measurements, the precision of measured results is impact. In some cases the ISFET sensor can work only in a given range of pH value.

Sources of errors of non-chemical causes includes:

Sensor wiring and electromagnetic fields – potentiometric sensors like ISFET are sensitive to electromagnetic field interferences which present in the environment, so that the grounding loops of measuring system become quite important. Such a

interference has a huge contribution in sensor drift must be avoided.

Ambient light and temperature – dark box and constant temperature control are essential to reduce the errors of measurement. Fortunately, ISFET behaves with excellent linearity, which makes the temperature compensation very easy.

3.4.2 Measurement setup

HP-4156 is used as measurement tool in this experiment. All experiment proceeds in the dark-box, to avoid the light emission causes the electron-hole pair in the semiconductor and the unknown results in the sensing membrane.

The electrolyte buffer solutions were purchased form Riedel-deHaen and the pH-value is 1, 3, 5, 7, 9, 11, 13, respectively. First of all, we glued a container made by plastic on the wafer, which is covered the sensing layer, and the container's volume is about 50 c.c. This step was important and complex, right here, an acknowledgement must be given for 3M company by the fine glue to reduce the glue proceed complexity.

A reference electrode is immersed in the electrolyte solution, to give the voltage to the EIS system same as the gate voltage controller in MOSFET. Where we fix the height from sensing layer surface to the reference electrode is trying to stabilize the electrical potential floating phenomenon. [7] Note that, the electrolyte must be injected into the container smoothly preventing the bubble produced near the sensing area.

Firstly, the electrical characteristic of drain current-voltage relation is used to determinate the FET quality. Fortunately, the device made in this work has a fine electrical property Fig.3.1. Next, the electrical relation between drain-current and gate-voltage is going on. The electrical characteristic of Id-Vg is used to determinate

the ISFET sensitivity. Electrolyte solutions change from the degree of pH=13 to the degree of pH=1 during the measurement of Id-Vg. We purpose the changing step of electrolyte by 3 times injecting and 3 times pumping to prevent the ion concentration over the fixed pH. When next to the following pH solution, first pumping electrolyte, and first injecting the target pH solution into container till the third injecting stop.

Secondly, the drift characteristic is measured with specific pH value of 7 and different sampling period of 30 seconds, 1 minute, 10 minutes and 1 hour. 33 sampling points in the time frame of 7 hours for each ISFET film.

3.5 References

[1]P. Bergveld, “Thirty years of ISFETOLOGY What happened in the past 30 years and what may happen in the next 30 years” Sensors and Actautors B 88 (2003)1-20

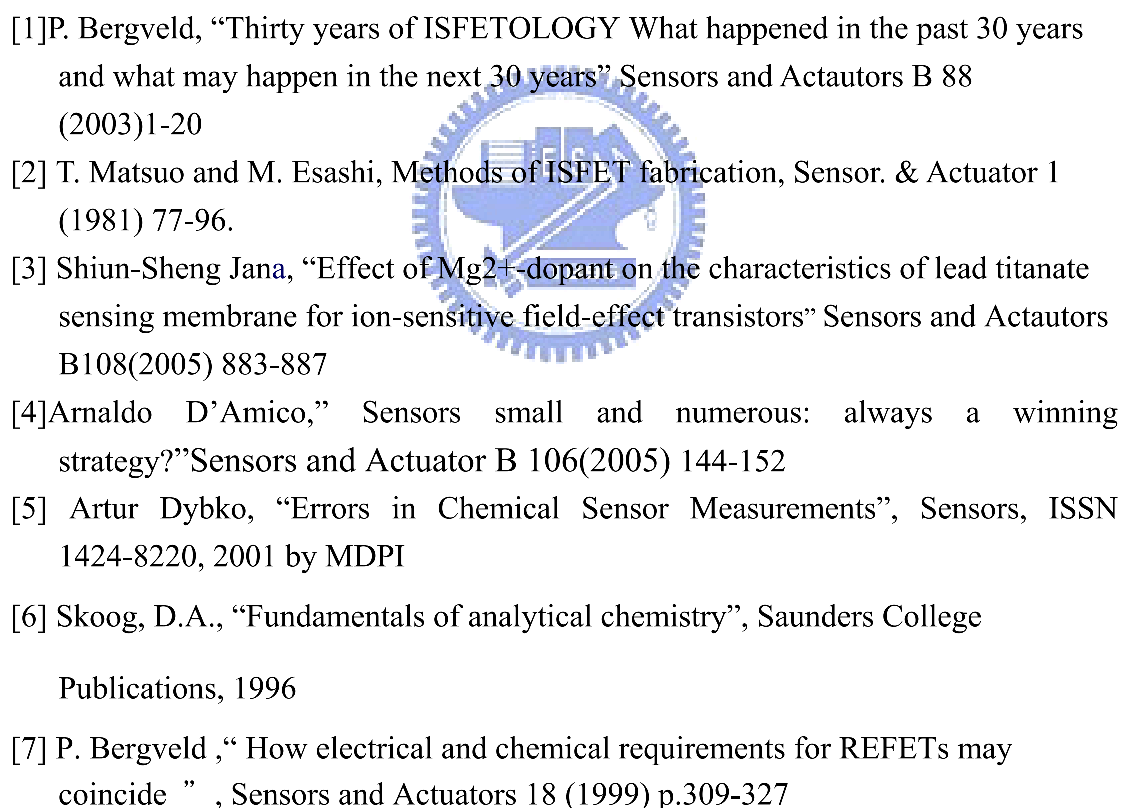

[2] T. Matsuo and M. Esashi, Methods of ISFET fabrication, Sensor. & Actuator 1 (1981) 77-96.

[3] Shiun-Sheng Jana, “Effect of Mg2+-dopant on the characteristics of lead titanate sensing membrane for ion-sensitive field-effect transistors” Sensors and Actautors B108(2005) 883-887

[4]Arnaldo D’Amico,” Sensors small and numerous: always a winning strategy?”Sensors and Actuator B 106(2005) 144-152

[5] Artur Dybko, “Errors in Chemical Sensor Measurements”, Sensors, ISSN 1424-8220, 2001 by MDPI

[6] Skoog, D.A., “Fundamentals of analytical chemistry”, Saunders College Publications, 1996

[7] P. Bergveld ,“ How electrical and chemical requirements for REFETs may coincide ” , Sensors and Actuators 18 (1999) p.309-327

Chapter 4

Results and Discussions

4.1 Introduction

The pH-ISFET differs from a MOSFET on the structural components especially in the gate terminal part. At which, the metal covered over gate material is replaced by electrolyte solution and a reference electrode. Changing the pH values of the electrolyte produces a potential drop which is differ from each value, thus, the sensitivity is arising when increasing pH value. In the point of view, determining the potential drop, expect the electrolyte, several kinds of sensing membrane is considered. In this work, titanium dioxide (TiO_2) and zirconium dioxide (ZrO_2) are used to be the sensing membrane because of the higher sensitivity and the stable electrical characteristic.

The pH-ISFET, a potentiometric based sensor, also needs a reference field-effect-transistor (REFET) to eliminate the other affecting factors, such as temperature effects. In our experiment, differs from others, trying to co-manufacturing ISFET/REFET in the CMOS processing by the method of purposed plasma surface treatment. To reduce the sensitivity, several time intervals by plasma treatment we tried. Finally, high/ low sensitivities of membranes for ISFET and REFET are essential for getting higher resolution of pH measurement.

4.2 Sensitivity characteristic of sensing materials

In changing of the sensing membrane, the sensitivity differs from each other because of the different characteristics of the sensing membrane. And we knew TiO_2 and ZrO_2 membranes have stable electric characteristic. Firstly, we discuss the sensitivity of pure sensing membrane. Next, the plasma treated sensing membrane is discussed. Each of them treats under NH_3 plasma surface treatment during 0, 5, 10, 20, 30, and 60 minutes.

4.2.1 Sensitivity characteristic of TiO_2 membrane

The sensitivity of pure TiO_2 membrane is the values of 56.7mV/pH, 58.3mV/pH, and 55mV/pH. It is presenting the stable sensitivity characteristic. And because of the better performance of TiO_2 in previous study investigated by our team, the TiO_2 membrane is used to be sensing membrane directly while the surface pretreatment of plasma finished. Fig.4.1 is the corresponding I-V curves with no plasma treatment of TiO_2, and figure 4.2 is the corresponding sensitivity of TiO_2 without plasma treatment. The way we find out sensitivity here based on following steps, firstly we calculate the I-V curve of pH=13 in Fig.4.1, secondly we find the maximum conductance corresponding to the value of voltage from g-V curve of pH=13, finally we find the voltage value of pH=13 with maximum conductance and it's corresponding current value by I-V curve of pH=13, then the fixed current value correspond to it's own voltage value with each pH I-V curve, plotting in Fig.4.2 and finding the value of slope out, then we got the sensitivity value. Fig.4.3 is the I-V curves of TiO_2 with NH_3 plasma treatment during 5 minutes, the narrower interval is showed, Fig.4.4 shows the corresponding sensitivity of TiO_2 with plasma treatment during 5 minutes. Fig.4.5 shows the TiO_2 electrical characteristic with NH_3 plasma treating during 10 minutes, and Fig.4.6 shows the corresponding sensitivity of TiO_2 with NH_3 plasma treatment

during 10 minutes. Fig.4.7 shows the I-V curves of TiO_2 treated with NH_3 plasma during 20 minutes, and the corresponding sensitivity is shown in Fig.4.8. The I-V curves of TiO_2 membrane treated by NH_3 plasma during 30 minutes is shown in Fig.4.9 and the corresponding sensitivity is shown in Fig.4.10. Obviously, there is a downstair tendency when the treating time increasing. Fig.4.11 shows the I-V curves of NH_3 treating time during 60 minutes and the corresponding sensitivity is shown in Fig.4.12. The raising value of treating time during 60 minutes is considered by the increasing effective dangling bonds. Table 4.1 lists the corresponding sensitivity values and Fig.4.13 shows the tendency of various plasma treating time interval.

4.2.2 Sensitivity characteristic of ZrO_2 membrane

Fig.4.14 shows the I-V curves of ZrO_2 without plasma treatment and the corresponding sensitivity is shown in Fig.4.15. Fig.4.16 shows the I-V curves of ZrO_2 treated by NH_3 plasma during 5 minutes, the narrower interval can be seen, and the corresponding sensitivity is shown in Fig.4.17. Fig.4.18 shows the I-V curves of ZrO_2 treated by NH_3 plasma during 10 minutes and Fig.4.19 shows the corresponding sensitivity. Fig.4.20 shows the I-V curves of ZrO_2 with NH_3 plasma treatment during 20 minutes and sensitivity chart is shown in Fig.4.21. Fig.4.22 shows the I-V curves of ZrO_2 with NH_3 plasma treatment during 30 minutes and the corresponding sensitivity is shown in Fig.4.23. Fig.4.24 shows the I-V curves of ZrO_2 treated by NH_3 plasma during 60 minutes and the corresponding sensitivity is shown in Fig.4.25. Table 4.2 lists the corresponding sensitivity values and Fig.4.26 shows the tendency of various plasma treating time interval. We have the downstair tendency in NH_3 plasma treatment during longer spending time.

4.3 The coplanar ISFET/REFET sensor array system

The sensor array system is composed by the coupled sensing membrane without plasma treatment and with post-plasma-treatment after deposition. In this experiment, we use TiO_2 membrane without and with NH_3 post-plasma-treatment to form the ISFET/REFET sensor array system, and ZrO_2 membrane without and with NH_3 post-plasma-treatment as the ISFET/REFET sensor array system. Thus, the table 4.3 lists the difference of coplanar structure in TiO_2 membrane and table 4.4 lists the difference of coplanar structure in ZrO_2 membrane. Obviously, the difference of sensitivity increased with longer NH_3 plasma treating time. The highest value we have about 34.2 mV/pH made by ZrO_2 pair.

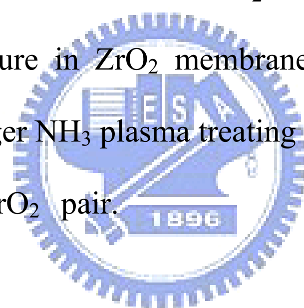

4.4 Conclusions

In this work, we are trying to study the influence factors with sensitivity and attending to simplify the manufacturing of REFET. For the further purpose, we are trying to realize the comanufacturing process of ISFET/REFET sensing array with compatible CMOS manufacturing process. And different from other gate materials of REFETs, the sensing materials are available in CMOS fabrication technology in this work. Fortunately, the purposed NH_3 plasma surface treatment work for the purpose indeed. A novel fabrication of REFET with plasma surface treatments is demonstrated.

And we have the sensitivity of co-planar structure of ISFET/REFET are 30.8mV/pH by TiO_2/NH_3_plasma_treated_30mins_TiO_2 and 34.2mV/pH by ZrO_2/NH_3_plasma_treated_60mins_ZrO_2.

Chapter 5

Future work

5.1 Future work

We had introduced the method of co-manufacturing ISFET/REFET by plasma treatment successfully in this work. Most of the attempts to create a REFET are based on covering the gate oxide of an ISFET with an additional ion insensitive membrane. Such as PVC membranes, but it is pity that they are not MOSFET fabrication compatible and the manufacturing of this material is complicated. So, the purposed methods of co-manufacturing ISFET/REFET are useful.

However, there still are lots of problems in ISFET. Such as the stability of sensing membrane, the reproducibility of ISFET (drift phenomenon), and the minification of ISFET. The minfication of ISFET is purposed by taking the solid state electrode replace the huge reference electrode immersed in the electrolyte.

Finally, based on the knowledge of ion-sensitive field effect transistor, the ion-selective field effect transistor can be produced by the same MOSFET manufacturing process. The ion-selective field effect transistor, resulted from sensing specific ions with the specific membrane, is also a proper extensive topic for future study.

Diameter (mm): 100+/-0.5
Type / Dopant : P / Boron
Orientation : <100>
Resistivity (ohm-cm):1-10
Thickness (μ m) ： 505-545
Grade : Prime

(a) Specifications of wafers

	TiO_2
Density	4.26
Z-ratio	0.4
Tooling	50.47
Current (mA)	1 ~ 60
Rate (Å/sec)	1.2
Pressure (Torr)	$5*10^{-6}$

(b) E – gun

parameters of ZrO_2 sputter
power : 200 W
Ar / O_2 : 24 / 8 (sccm)
Density : 6.51
Acoustic impendance : 14.72
Tooling factor : 0.533
Rate : 0.01 Å / s
pre sputter 60W for 10 min
Pressure : 7.6×10^{-3}

(c) Sputter

NH3
Pressure=200mtorr
RF power=100w
Flow rate=30sccm
Temperature=300℃

(d) Plasma

Table 3.1 (a) Specifications of wafers

(b) Parameters of sensing layers deposition with E – gun

(c) Parameters of sensing layers deposition with Sputter

(d) Condition of plasma treatment

Sensitivity (mV/pH)		1~7	7~13	1~13
TiO_2_NH_3 plasma treatment	0 min	58.3	53.3	55.8
	5 mins	61.7	41.7	51.7
	10 mins	55	20	61.7
	20 mins	40	25	32.5
	30 mins	28.3	16.7	22.5
	60 mins	30	30	30

Table 4.1 Sensitivity values of TiO2 with NH3 plasma treatment during time interval

Sensitivity (mV/pH)		1~7	7~13	1~13
ZrO_2_NH_3 plasma treatment	0 min	**63.3**	**61.7**	**62.5**
	5 mins	**60**	**51.7**	**55.8**
	10 mins	**58.3**	**50**	**54.2**
	20 mins	**56.7**	**60**	**58.3**
	30 mins	**56.7**	**31.7**	**44.2**
	60 mins	**0**	**10**	**5**

Table 4.2 Sensitivity values of ZrO2 with NH3 plasma treatment during time interval

Sensitivity(mV/pH)		1~7	7~13	1~13
TiO2-NH3 treated TiO2	5 mins	-3.4	11.6	4.1
	10 mins	3.3	23.3	18.3
	20 mins	18.3	28.3	23.3
	30 mins	30	36.6	30.8
	60 mins	28.3	23.3	25.8

Table 4.3 The sensitivity of coplanar structure in TiO_2 membrane

Sensitivity(mV/pH)		1~7	7~13	1~13
ZrO2-NH3 treated ZrO2	5 mins	6.7	1.6	4.2
	10 mins	3.4	28.3	15.8
	20 mins	6.7	23.3	15
	30 mins	11.7	36.6	24.2
	60 mins	28.4	40	34.2

Table 4.4 The sensitivity of coplanar structure in ZrO_2 membrane

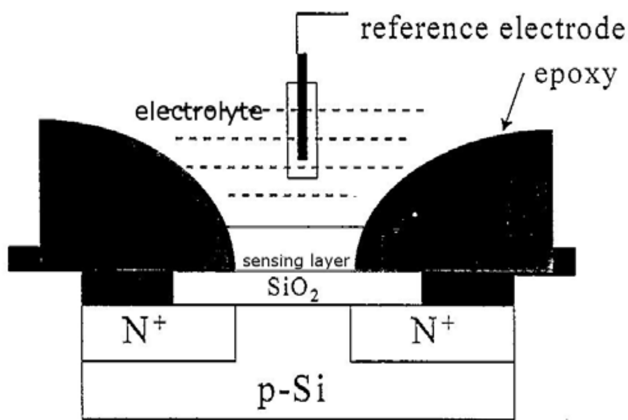

Fig 1.1 The schematic of ISFET

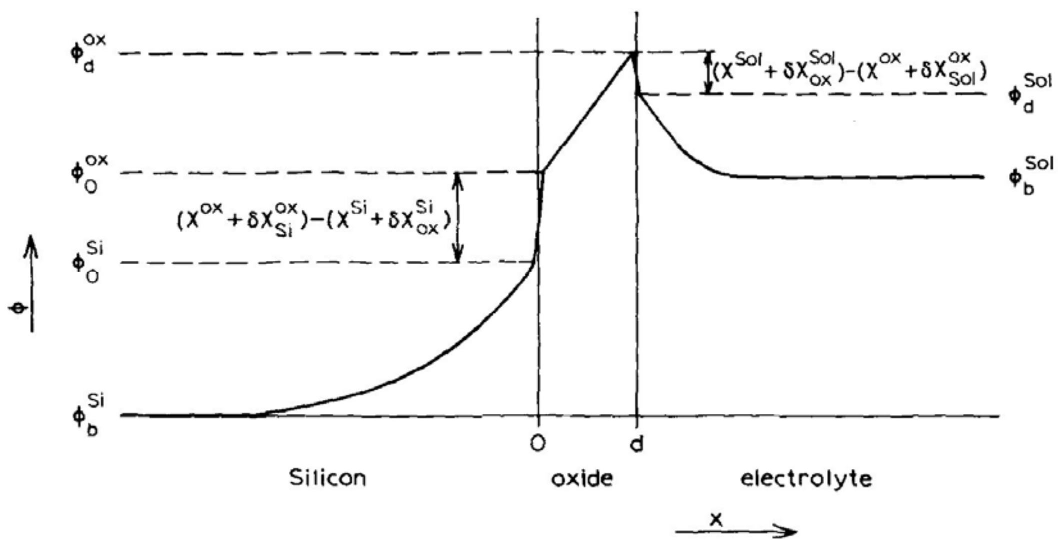

Fig 2.1 ISFET structure band diagram

(Luc Bousse, J. Chem. Phys. , 76)

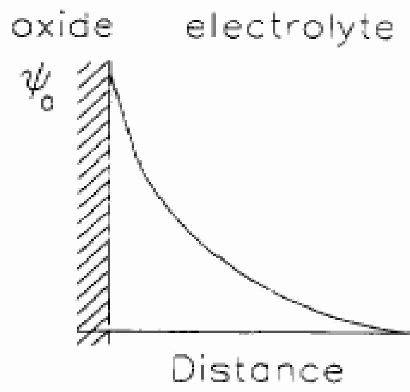

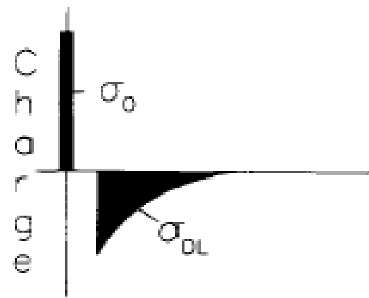

Figure 2.2 Potential profile and charge distribution at oxide / electrolyte interface

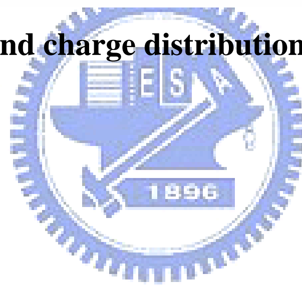

`

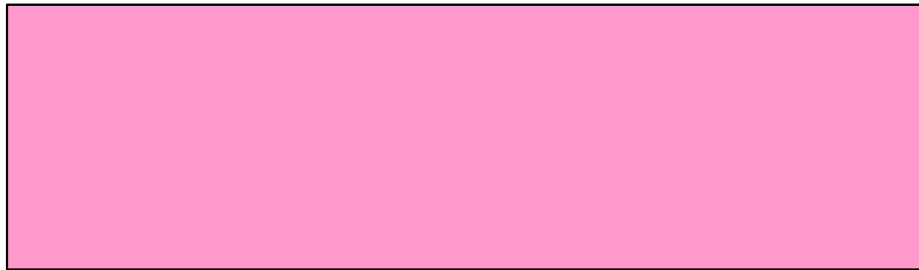

(a) RCA clean bare silicon

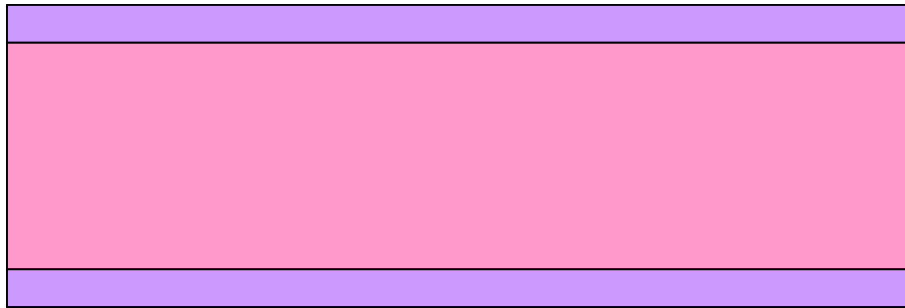

(b) wet oxidation

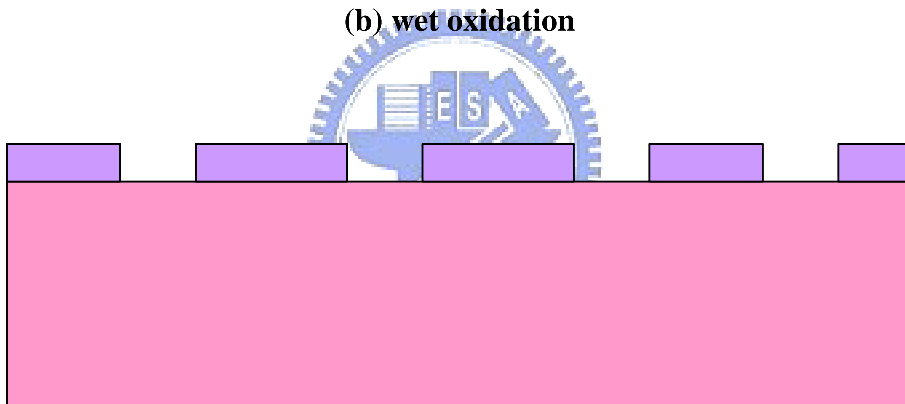

(c) mask Ⅰ

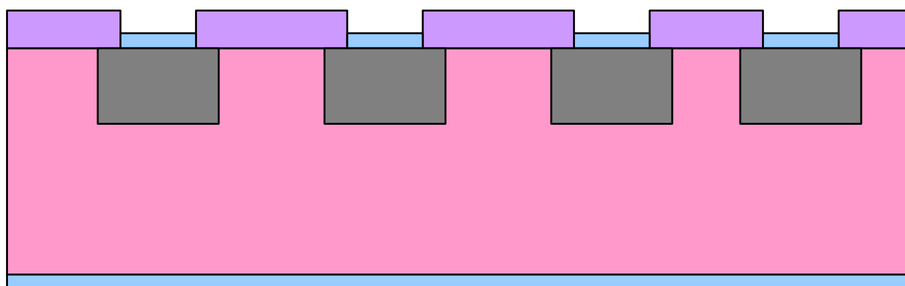

(d) screening oxidation & implantation

Figure 3.1 Experimental process

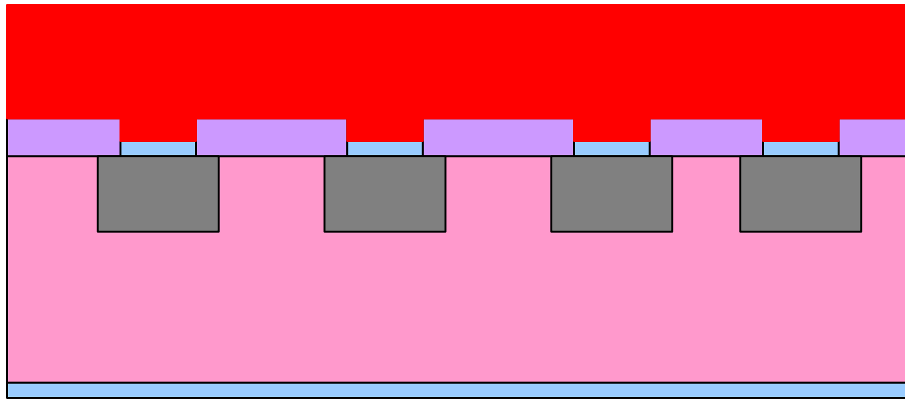

(e) passivation layer deposition

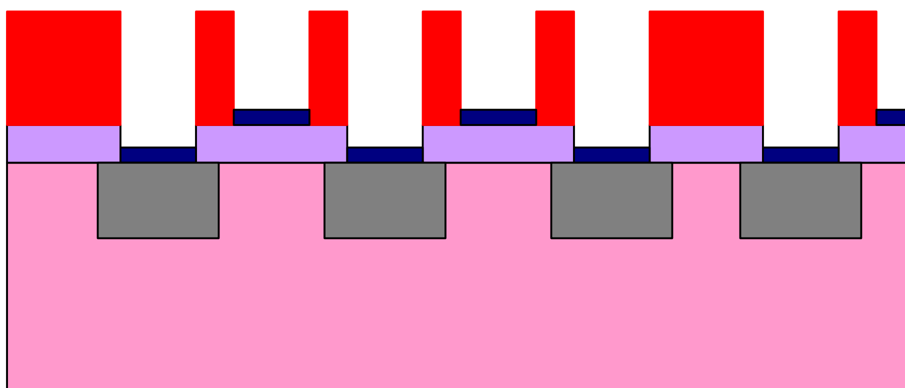

(f) mask II & dryoxidation

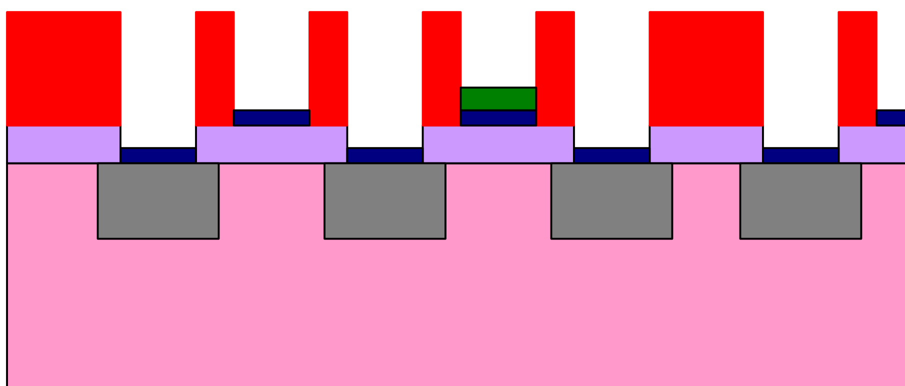

(g) sensing layer α deposition

Figure 3.1 Experimental process

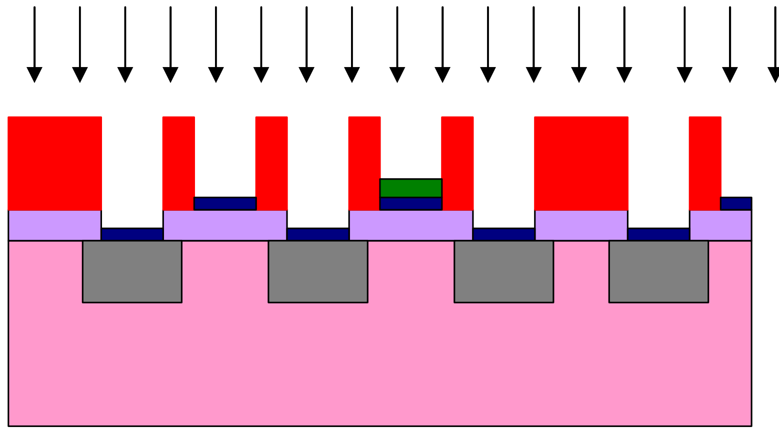

(i) Surface plasma treatment

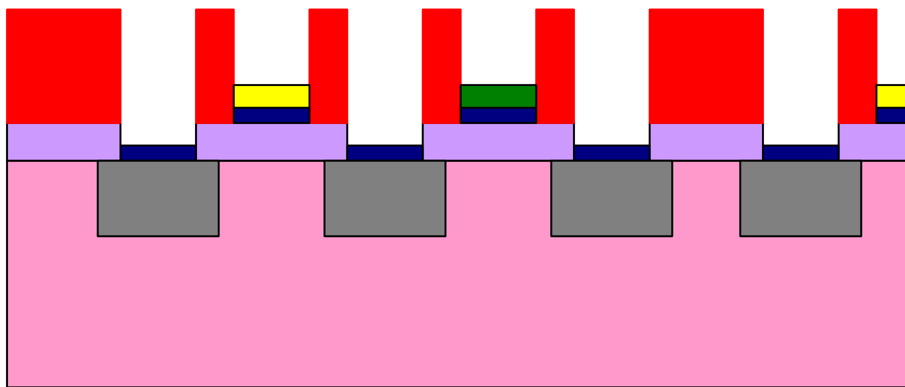

(j) Sensing layer *β* deposition & mask Ⅲ

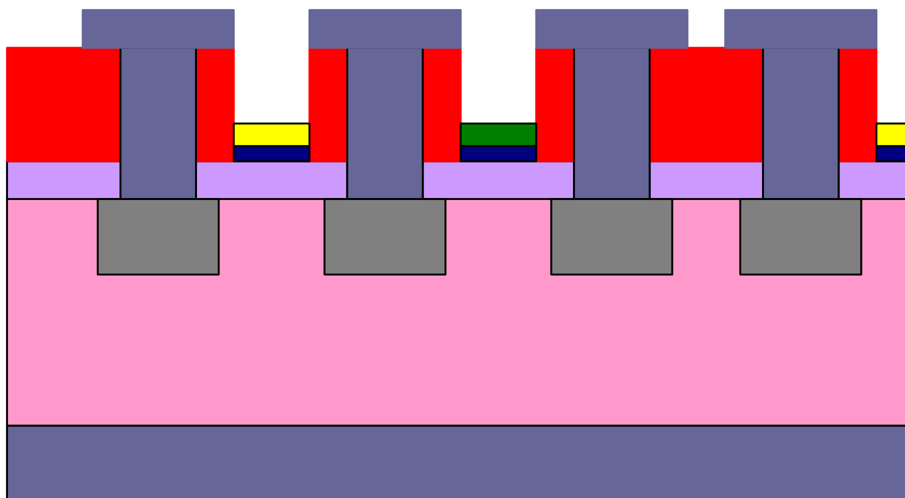

(k) Al deposition

Figure 3.1 Experimental process

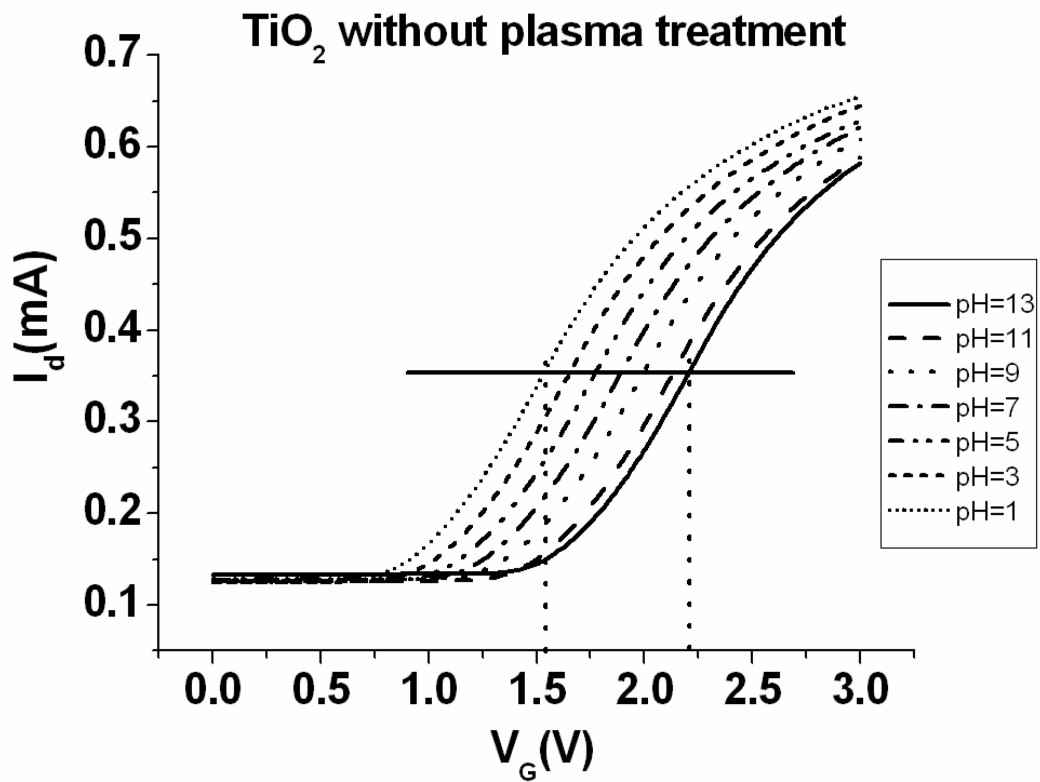

Fig 4.1 I-V curves of TiO2 without plasma treatment

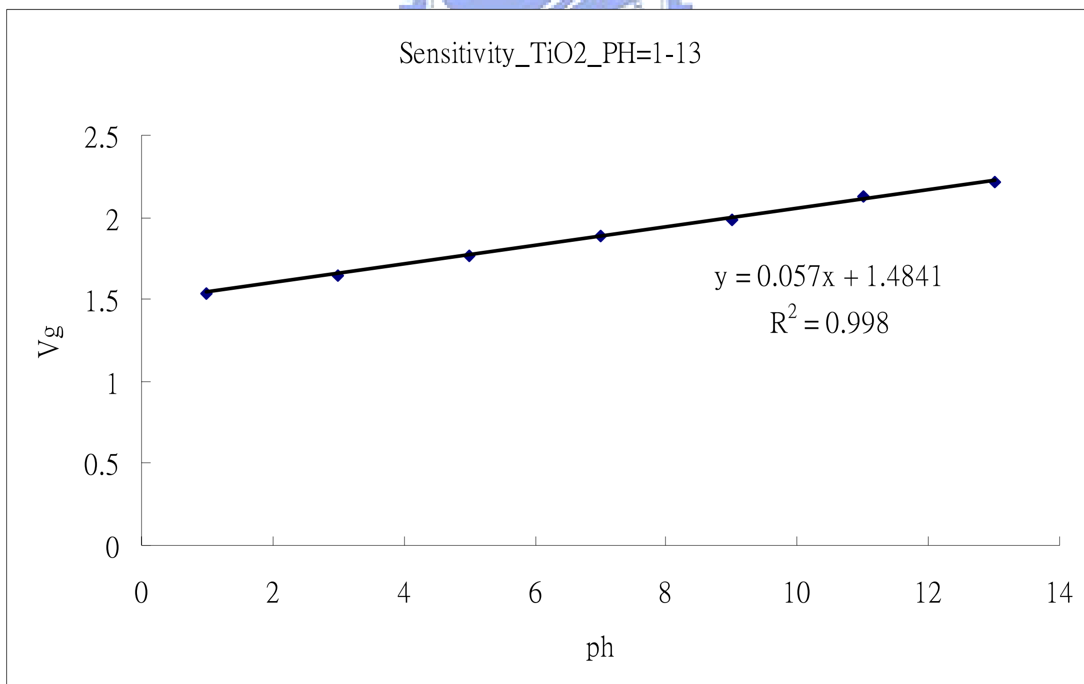

Fig 4.2 Sensitivity chart of TiO2 without plasma treatment

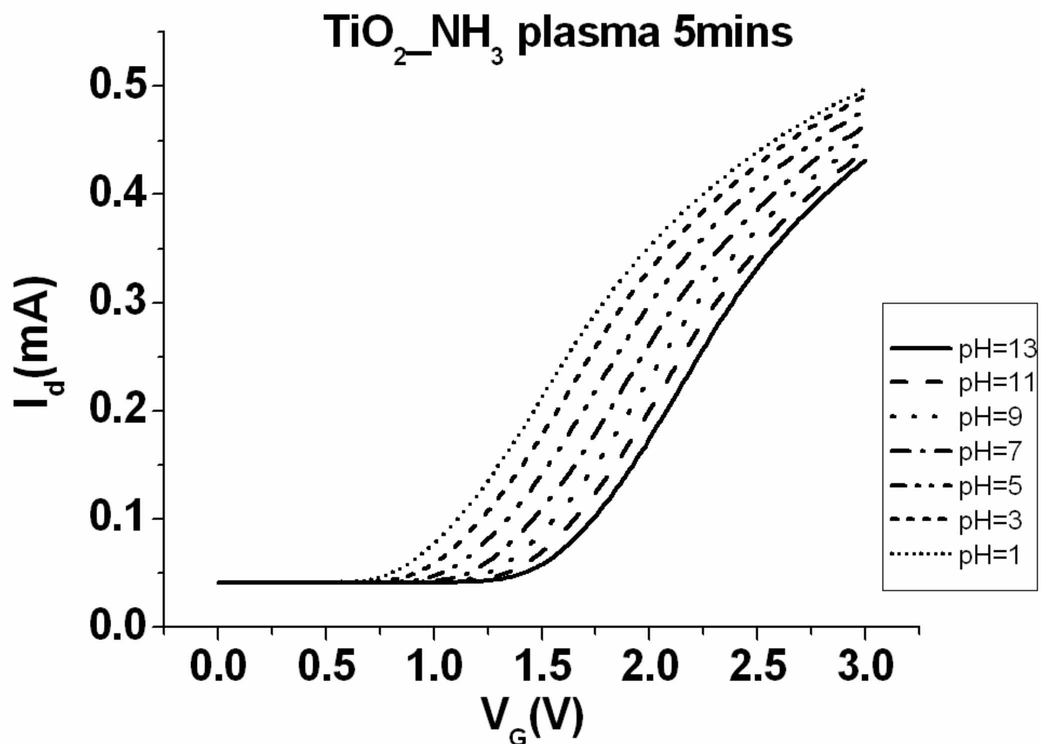

Fig 4.3 I-V curves of TiO_2 membrane with NH_3 plasma treatment during 5 minutes

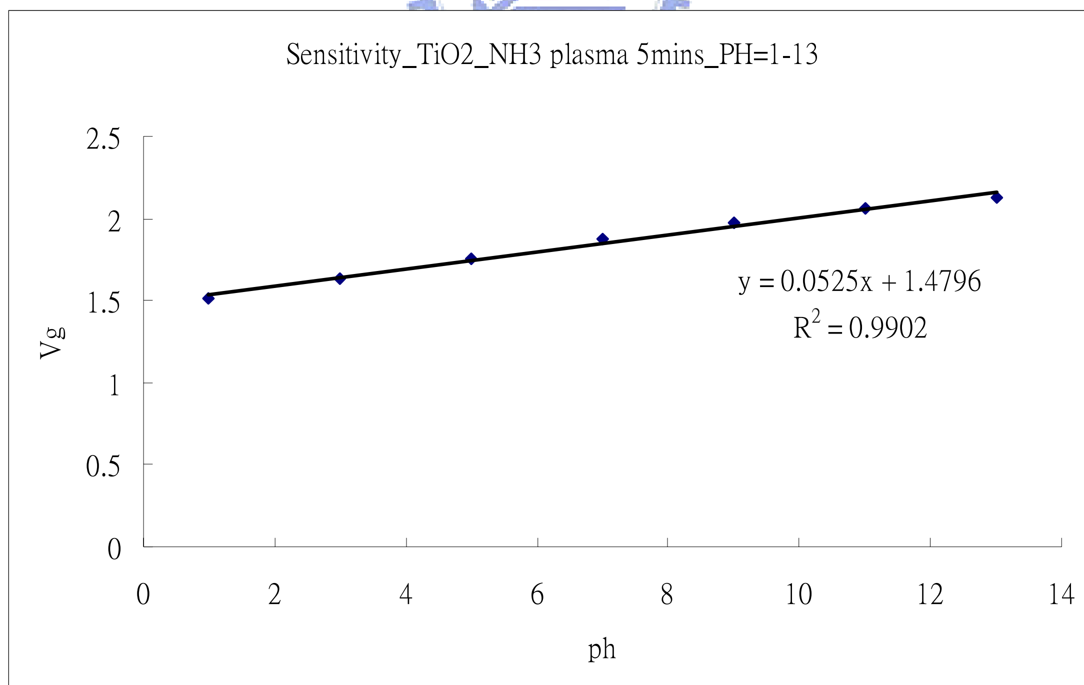

Fig 4.4 Sensitivity chart of TiO_2 with NH_3 plasma treatment during 5 minutes

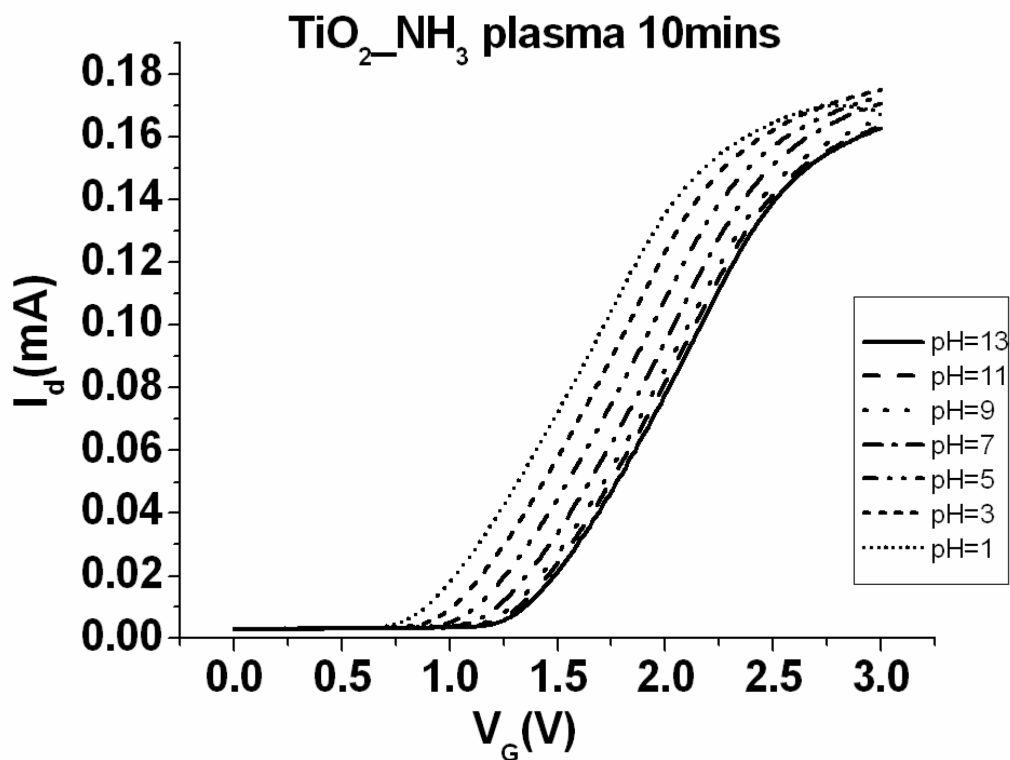

Fig 4.5 I-V curves of TiO_2 membrane with NH_3 plasma treatment during 10 minutes

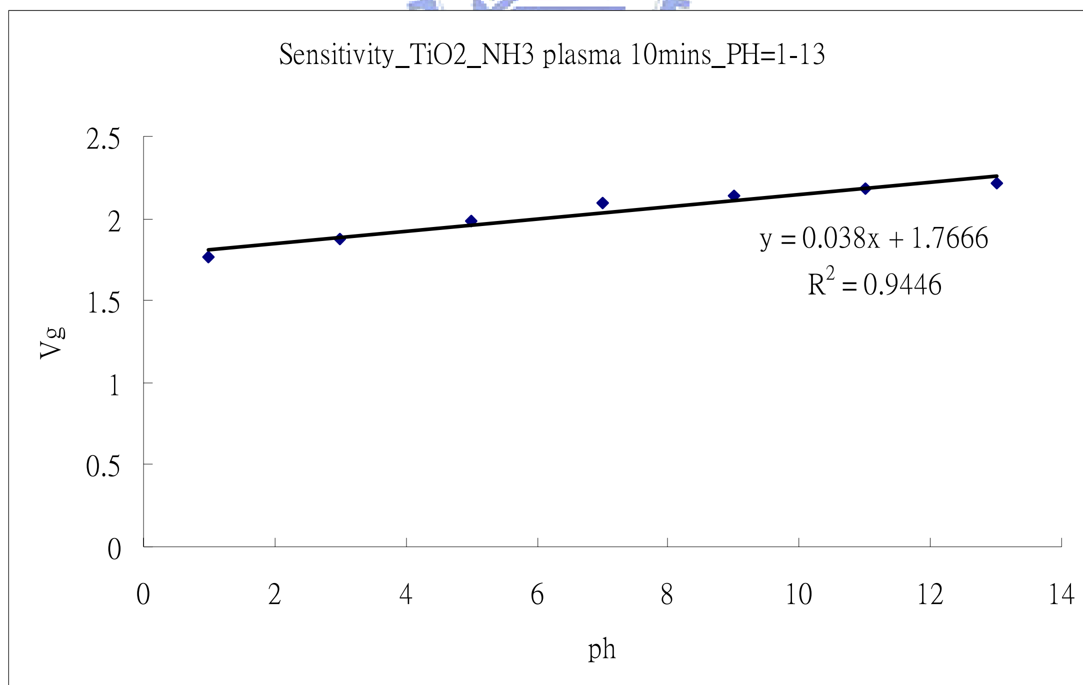

Fig 4.6 Sensitivity chart of TiO_2 with NH_3 plasma treatment during 10 minutes

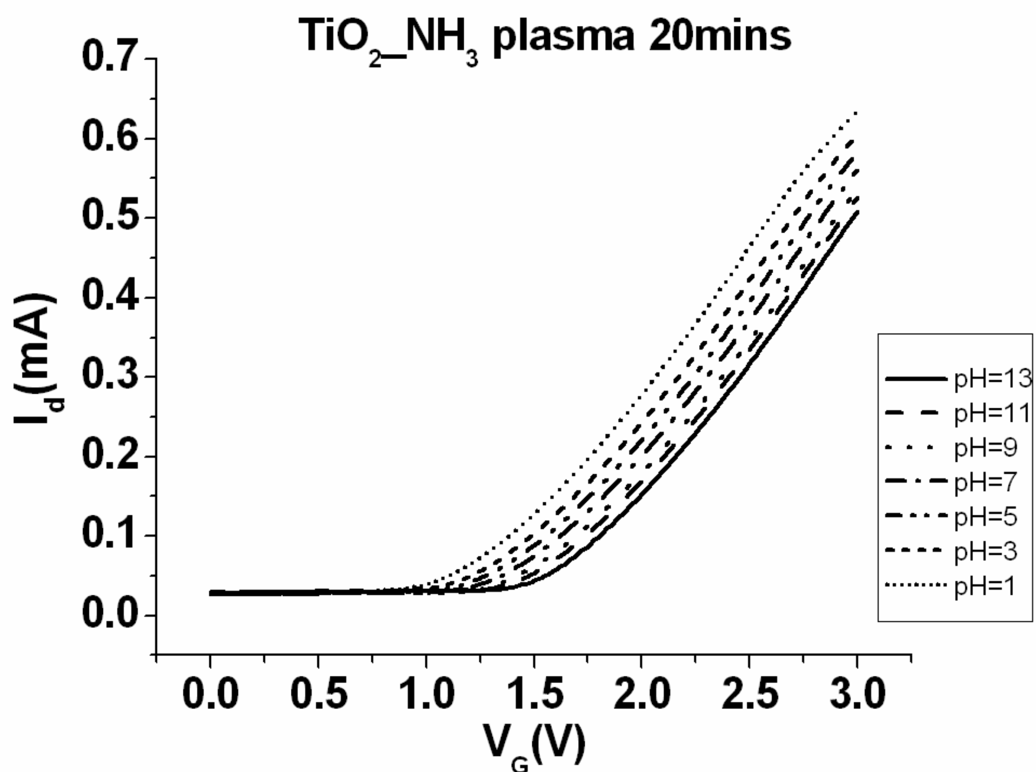

Fig 4.7 I-V curves of TiO_2 membrane with NH_3 plasma treatment during 20 minutes

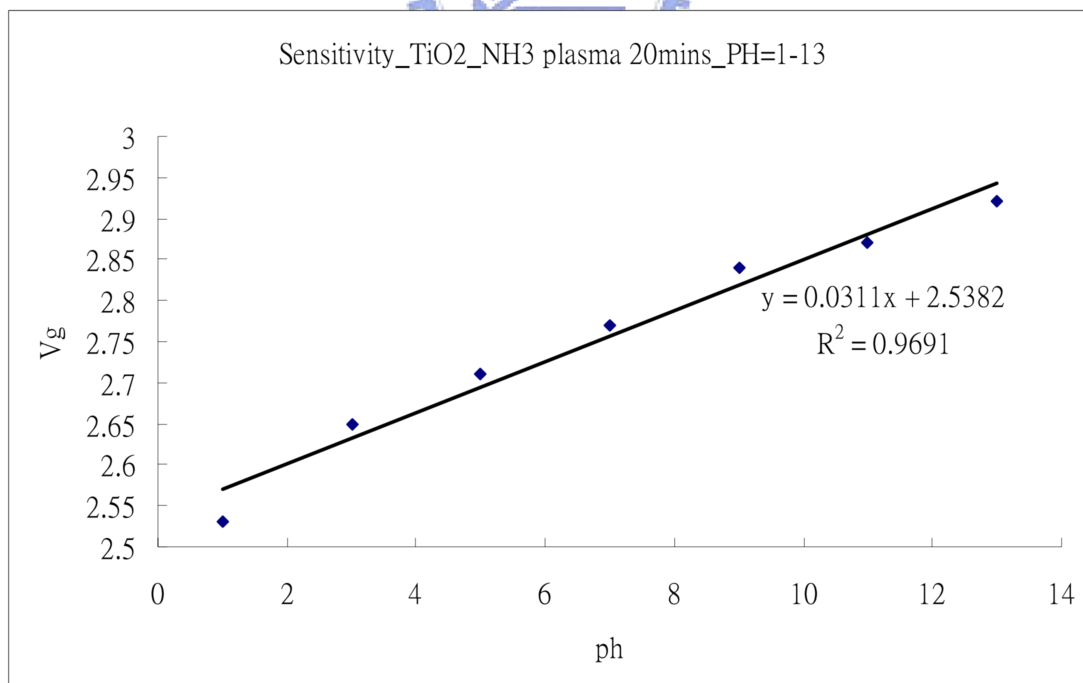

Fig 4.8 Sensitivity chart of TiO_2 with NH_3 plasma treatment during 20 minutes

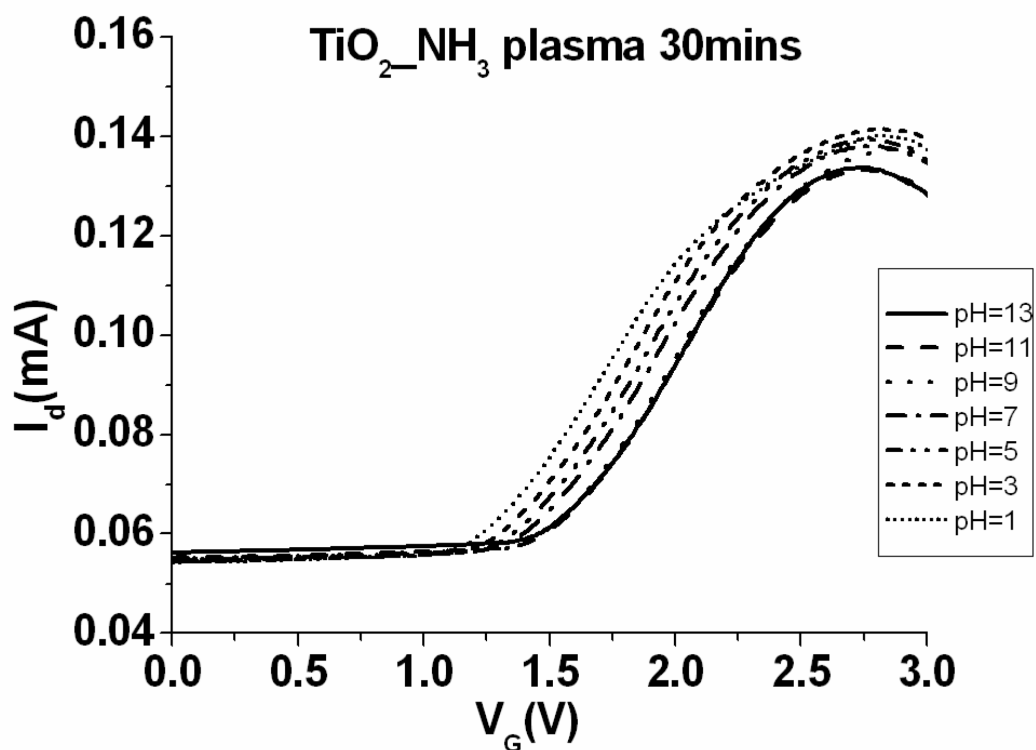

Fig 4.9 I-V curves of TiO_2 membrane with NH_3 plasma treatment during 30 minutes

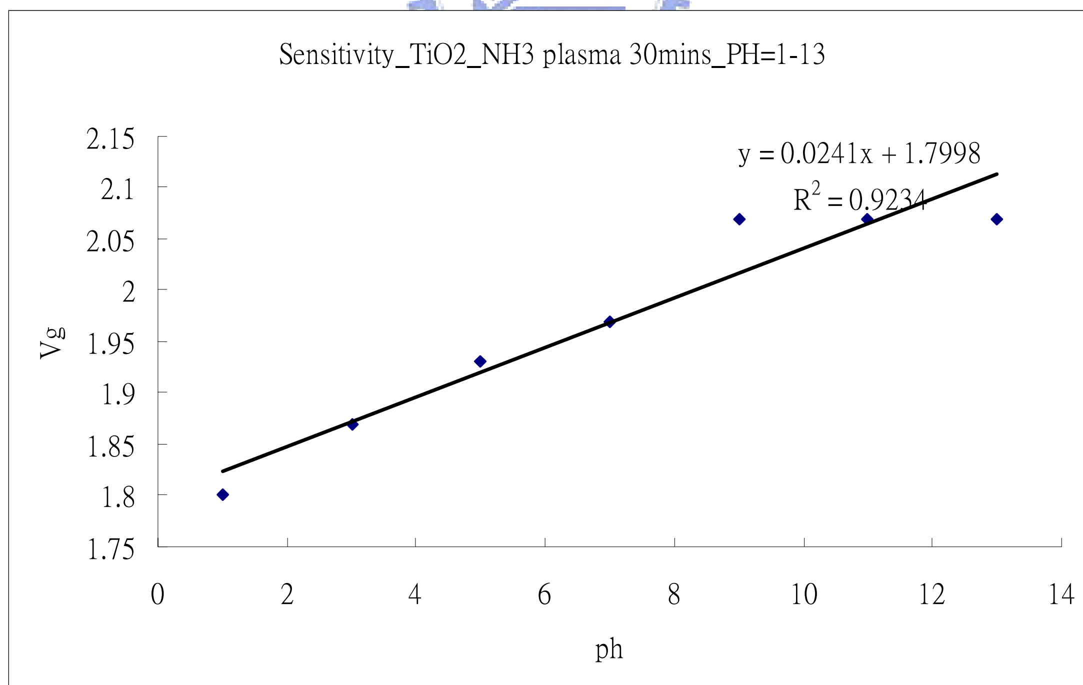

Fig 4.10 Sensitivity chart of TiO_2 with NH_3 plasma treatment during 30 minutes

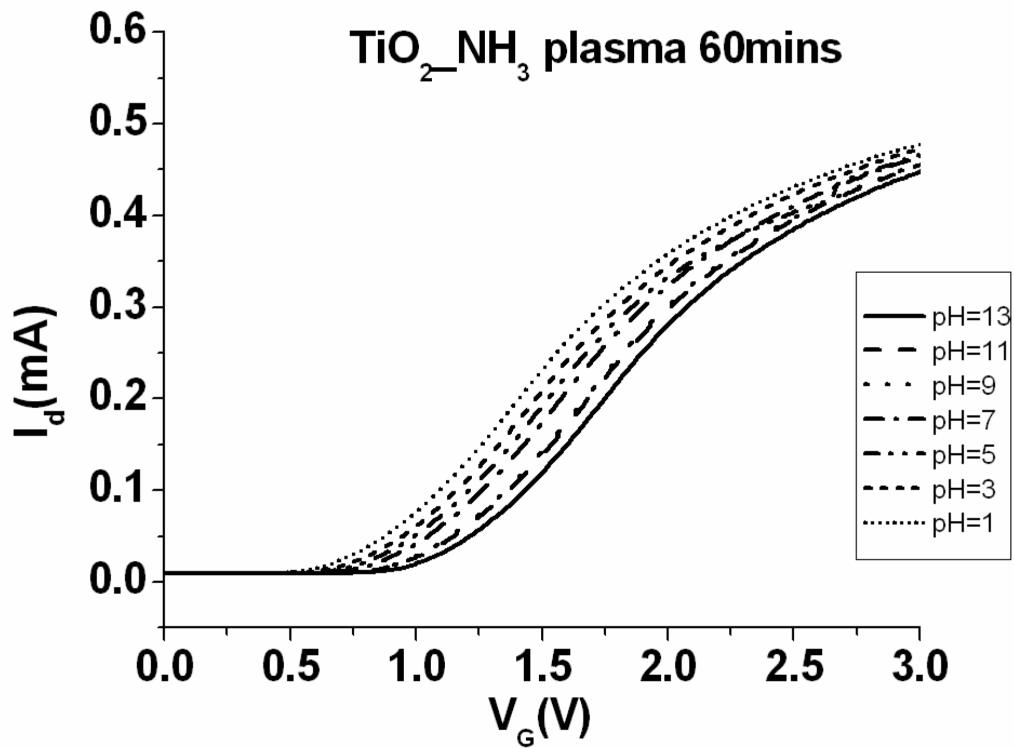

Fig 4.11 I-V curves of TiO_2 membrane with NH_3 plasma treatment during 60 minutes

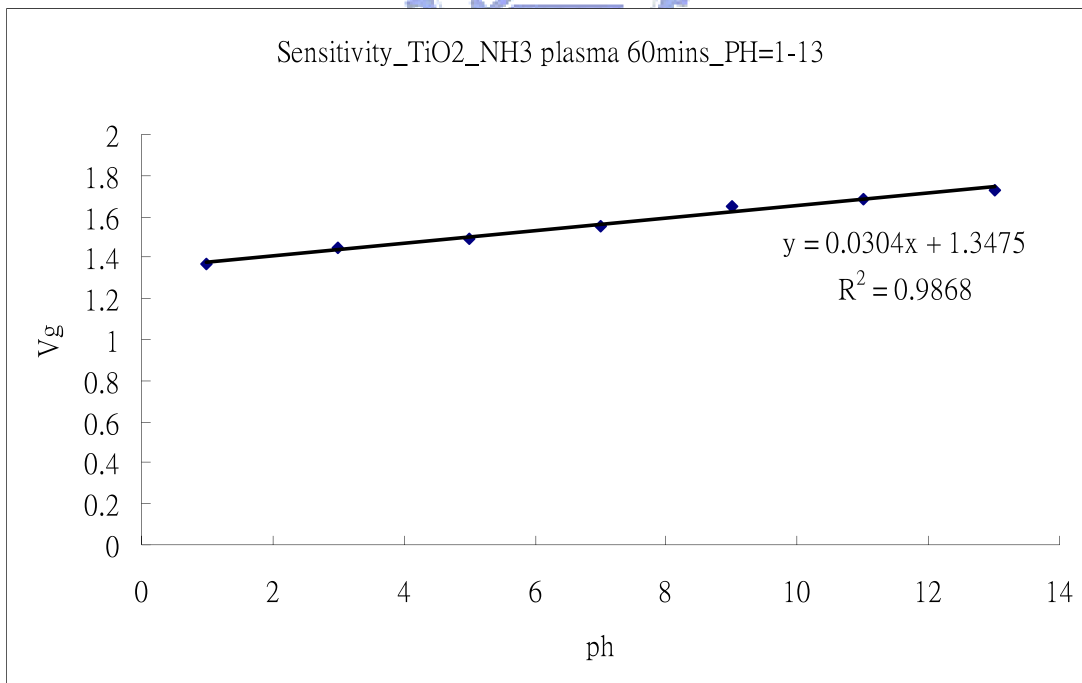

Fig 4.12 Sensitivity chart of TiO_2 with NH_3 plasma treatment during 60 minutes

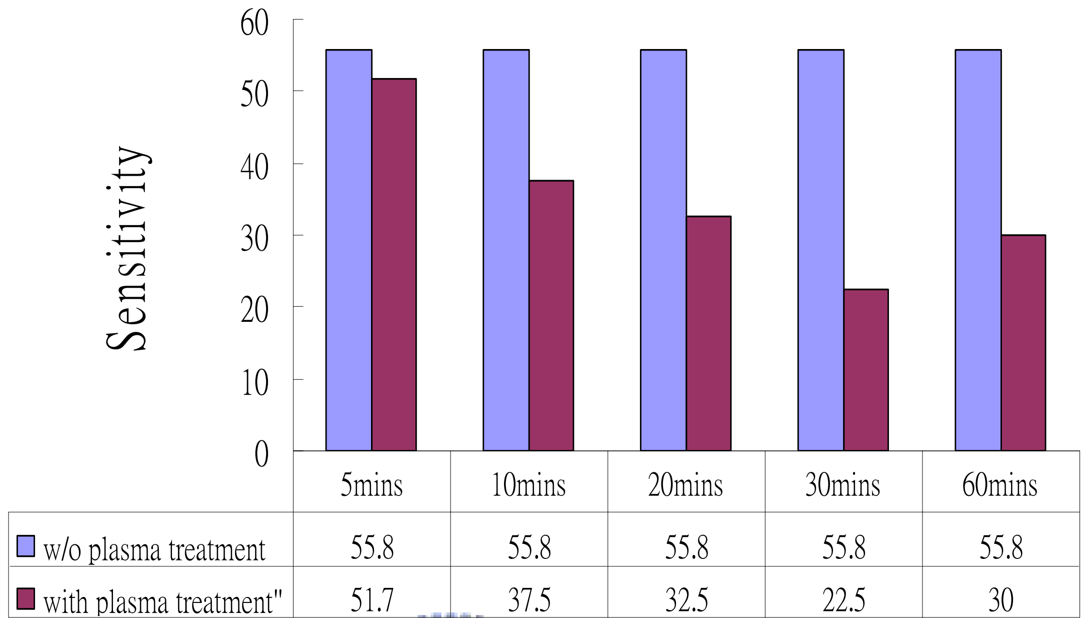

Fig 4.13 The tendency of various plasma treating time interval of TiO_2

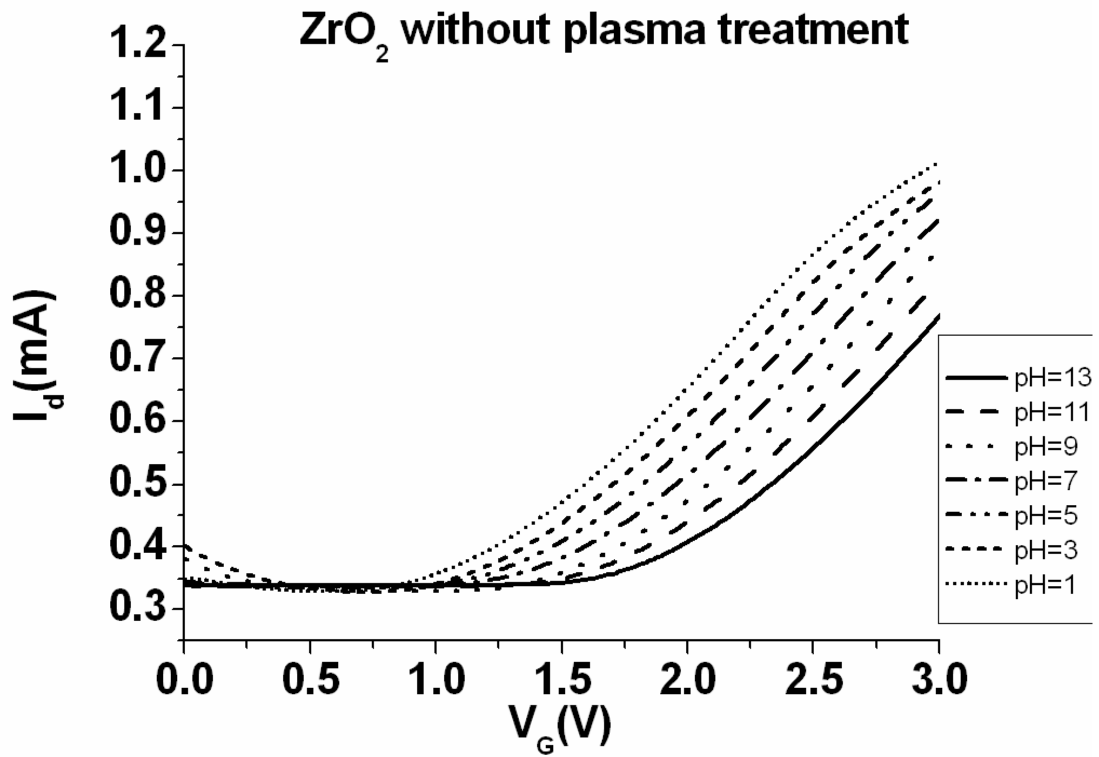

Fig 4.14 I-V curves of ZrO_2 without plasma treatment

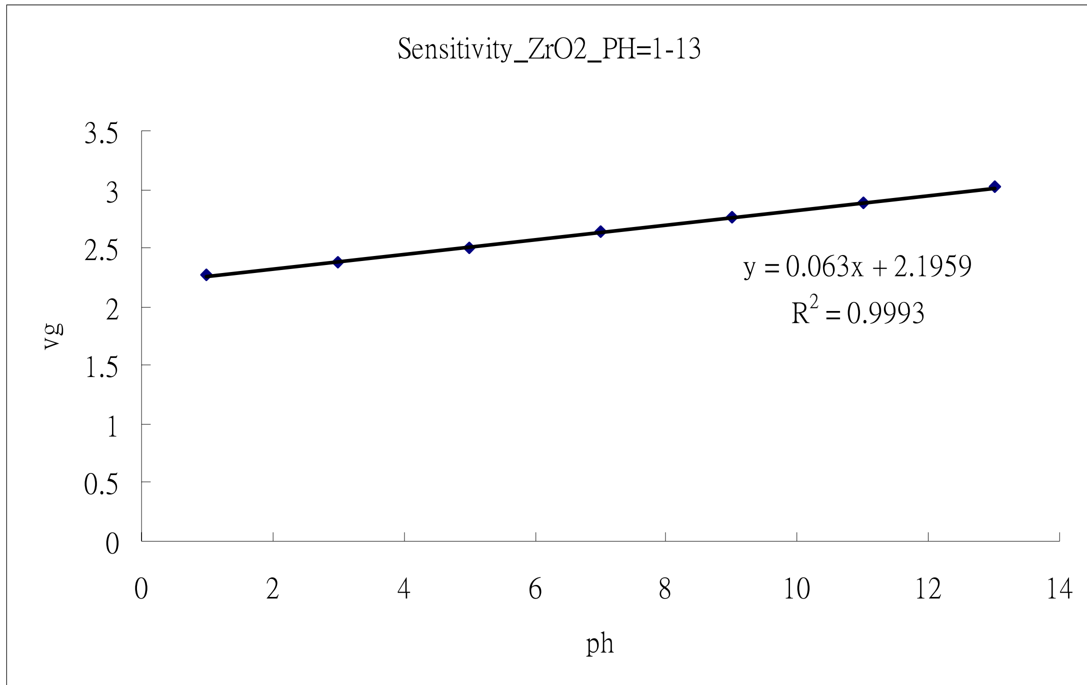

Fig 4.15 Sensitivity chart of ZrO_2 without plasma treatment

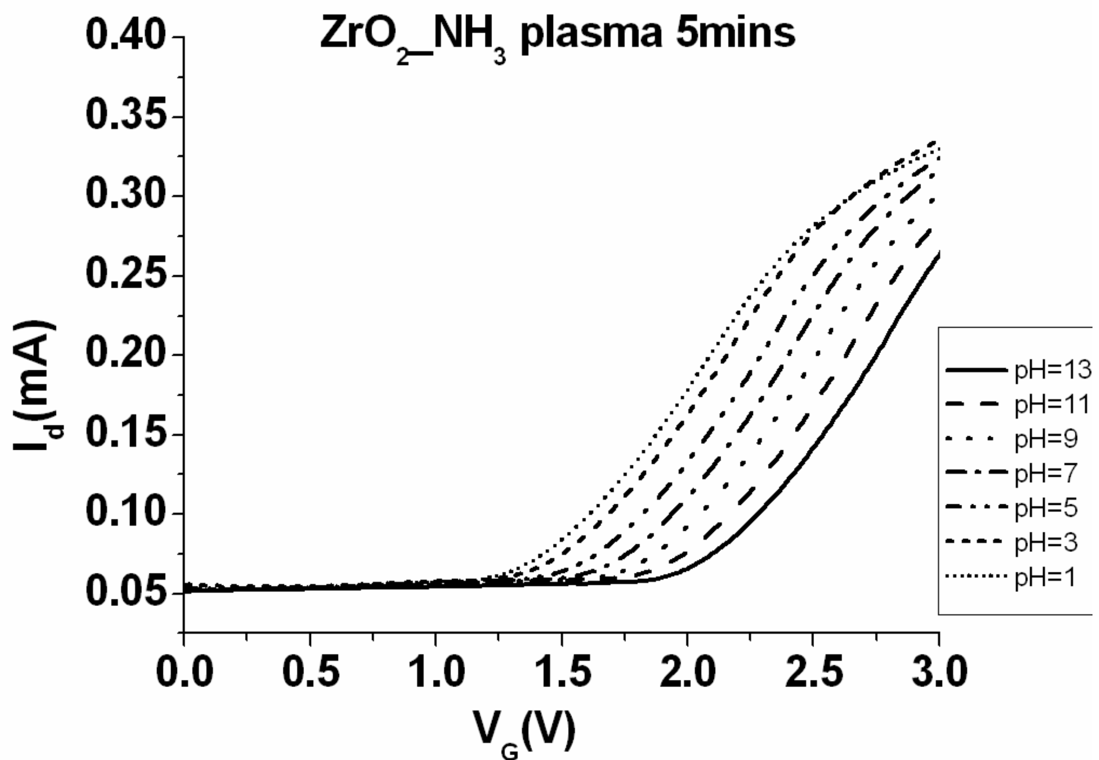

Fig 4.16 I-V curves of ZrO2 membrane with NH3 plasma treatment during 5 minutes

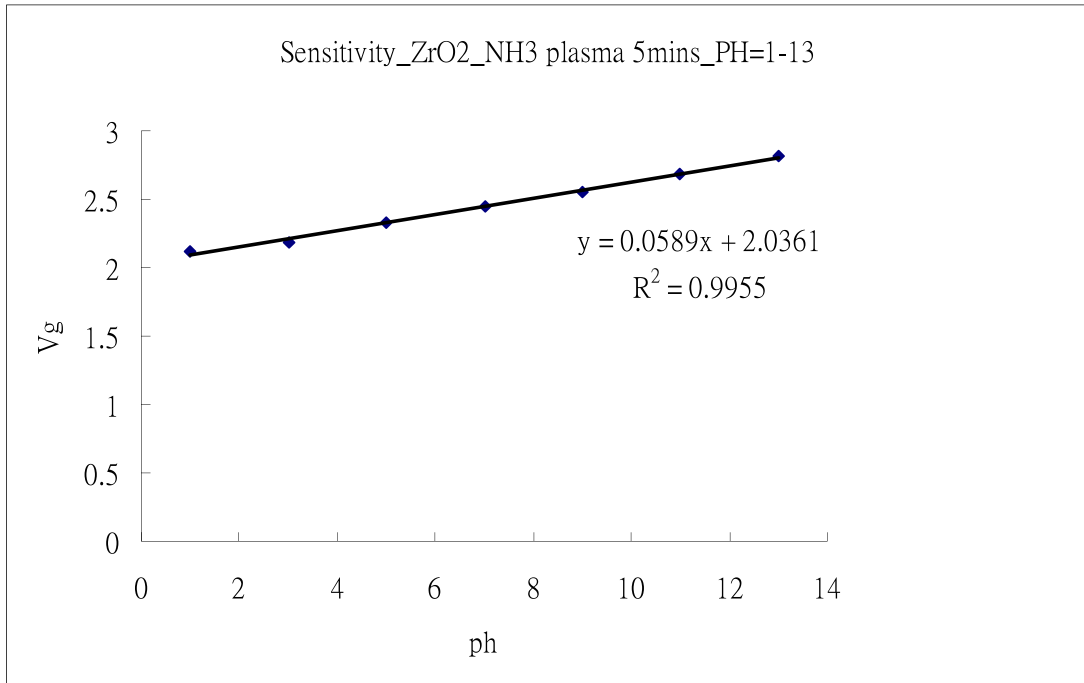

Fig 4.17 Sensitivity chart of ZrO_2 with NH_3 plasma treatment during 5 minutes

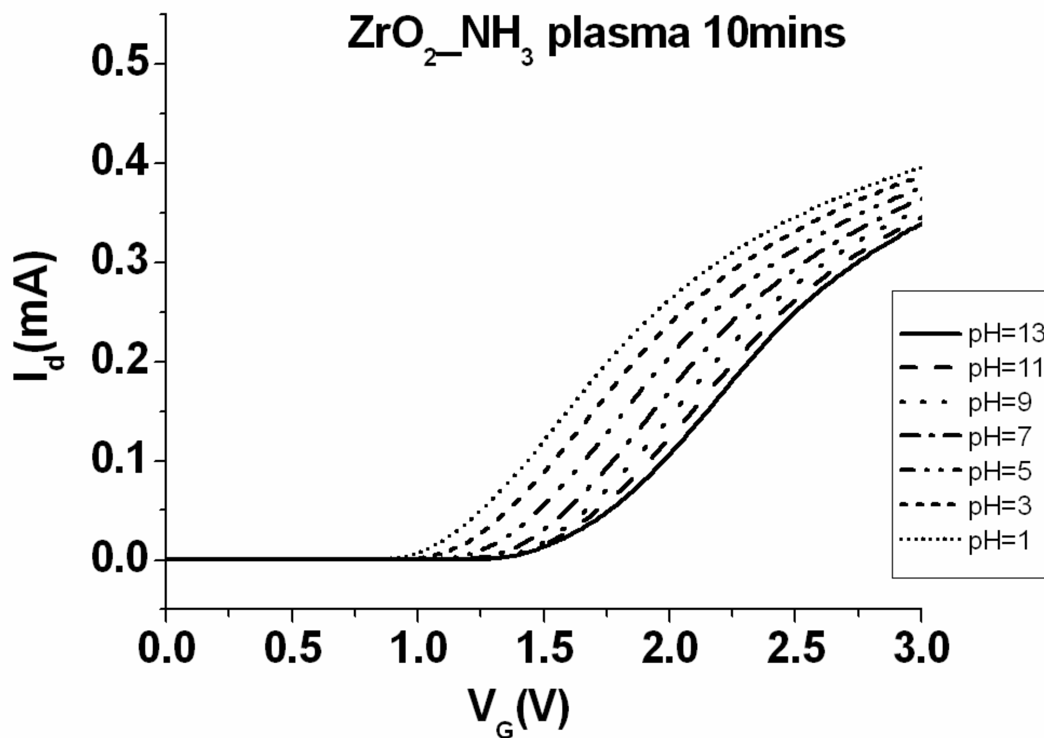

Fig 4.18 I-V curves of ZrO_2 membrane with NH_3 plasma treatment during 10 minutes

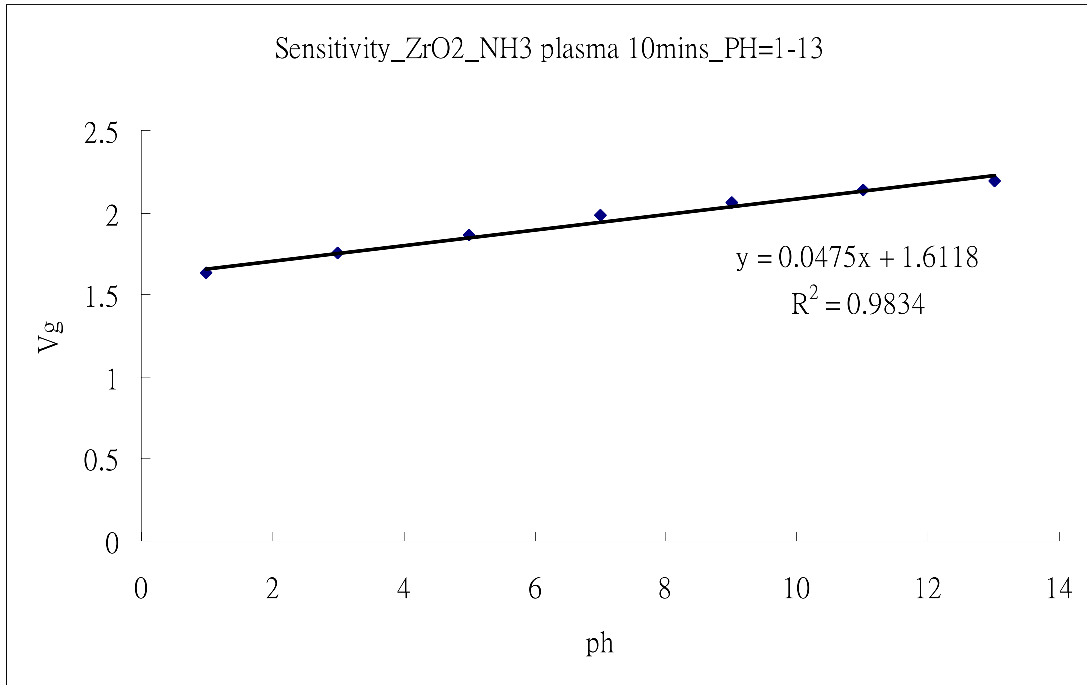

Fig 4.19 Sensitivity chart of ZrO_2 with NH_3 plasma treatment during 10 minutes

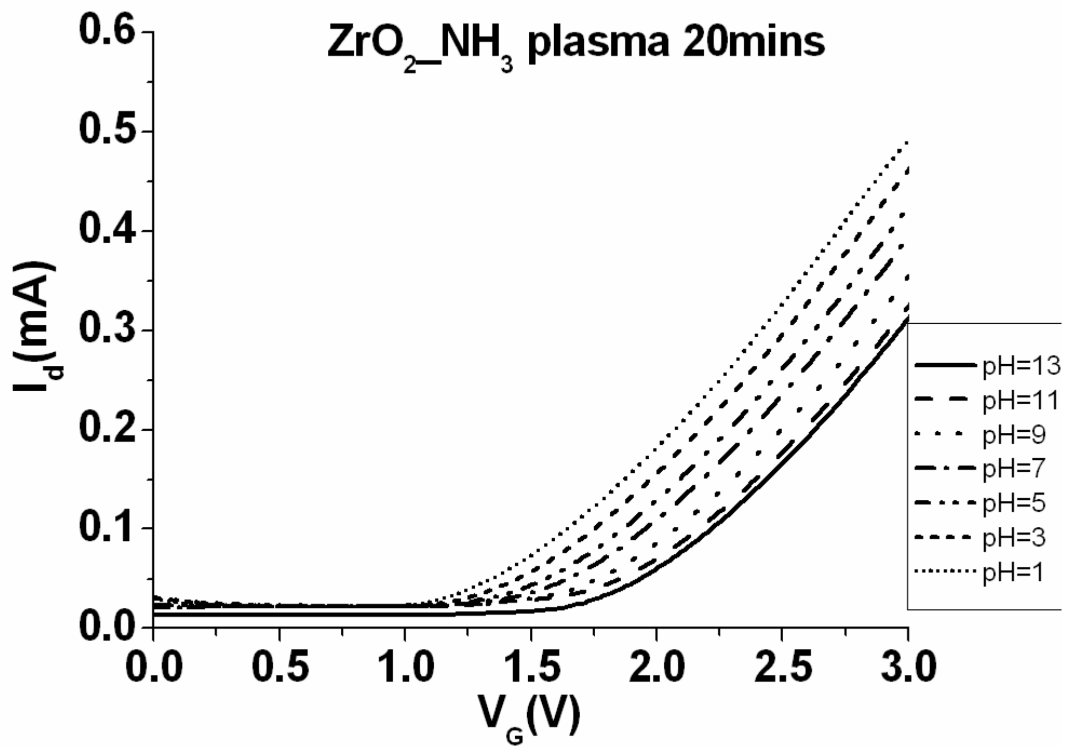

Fig 4.20 I-V curves of ZrO_2 membrane with NH_3 plasma treatment during 20 minutes

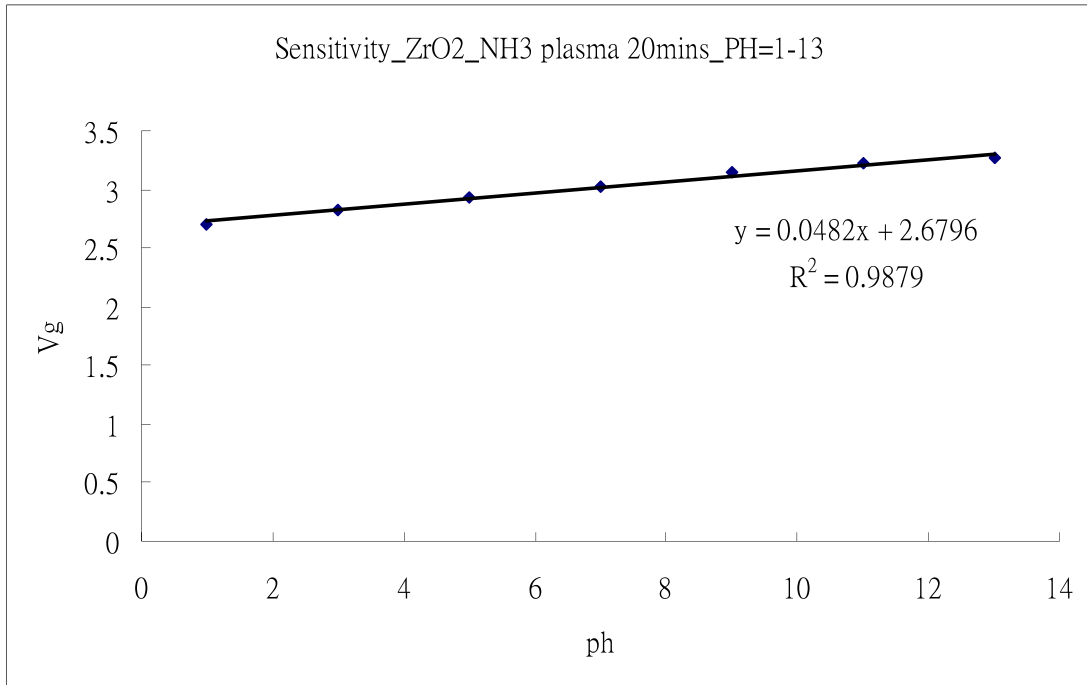

Fig 4.21 Sensitivity chart of ZrO_2 with NH_3 plasma treatment during 20 minutes

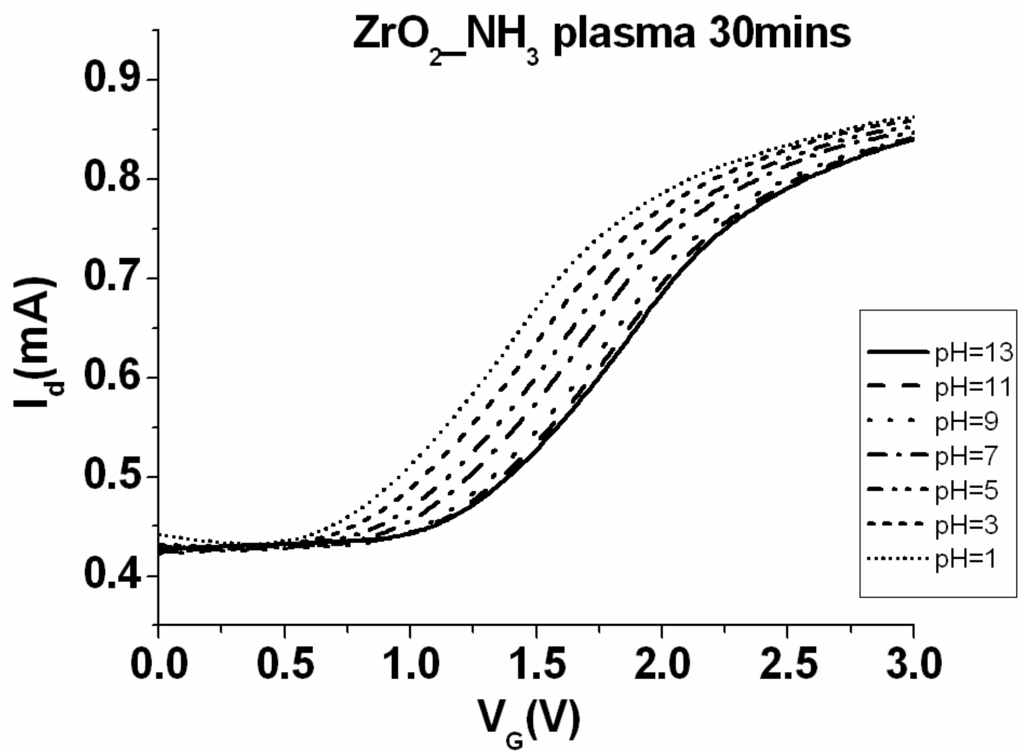

Fig 4.22 I-V curves of ZrO_2 membrane with NH_3 plasma treatment during 30 minutes

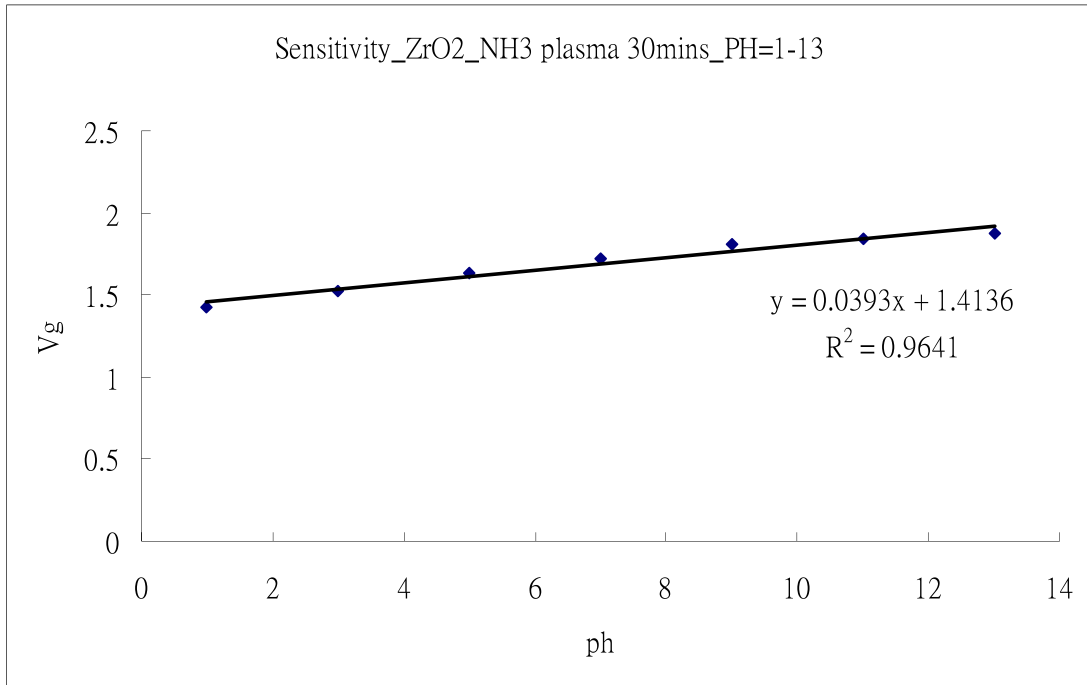

Fig 4.23 Sensitivity chart of ZrO_2 with NH_3 plasma treatment during 30 minutes

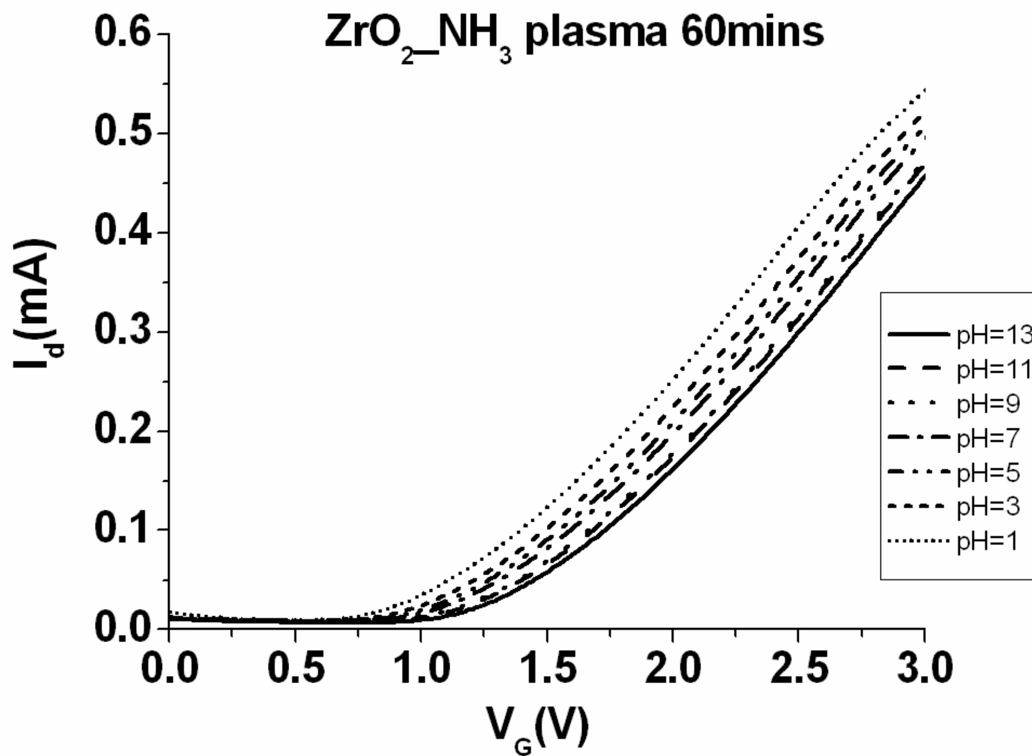

Fig 4.24 I-V curves of ZrO_2 membrane with NH_3 plasma treatment during 60 minutes

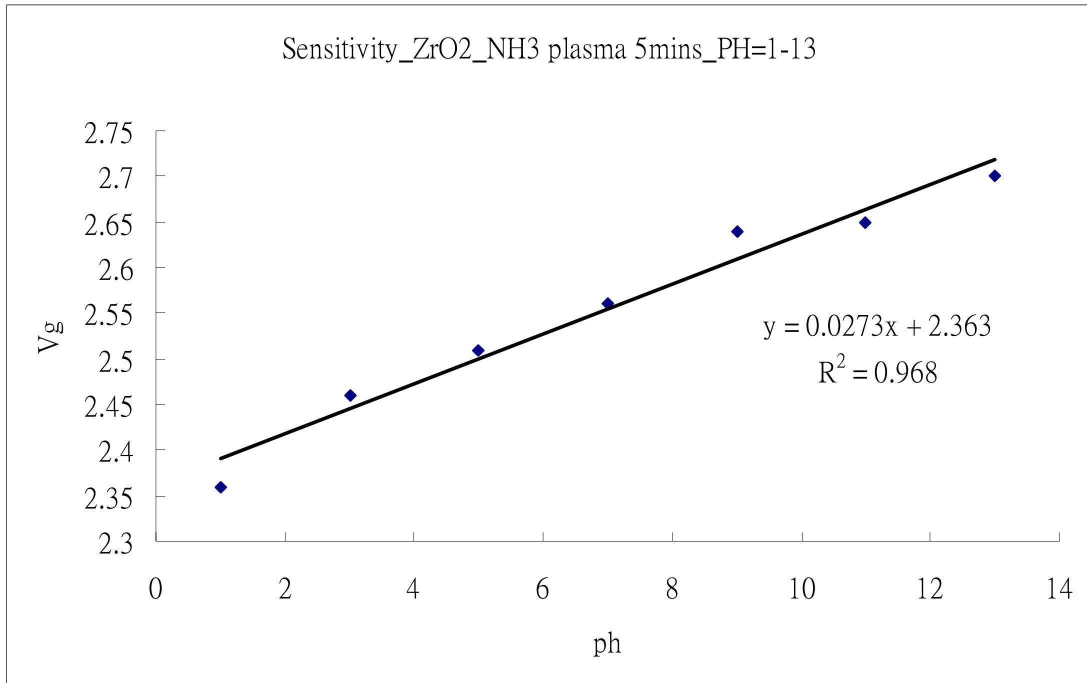

Fig 4.25 Sensitivity chart of ZrO_2 with NH_3 plasma treatment during 60 minutes

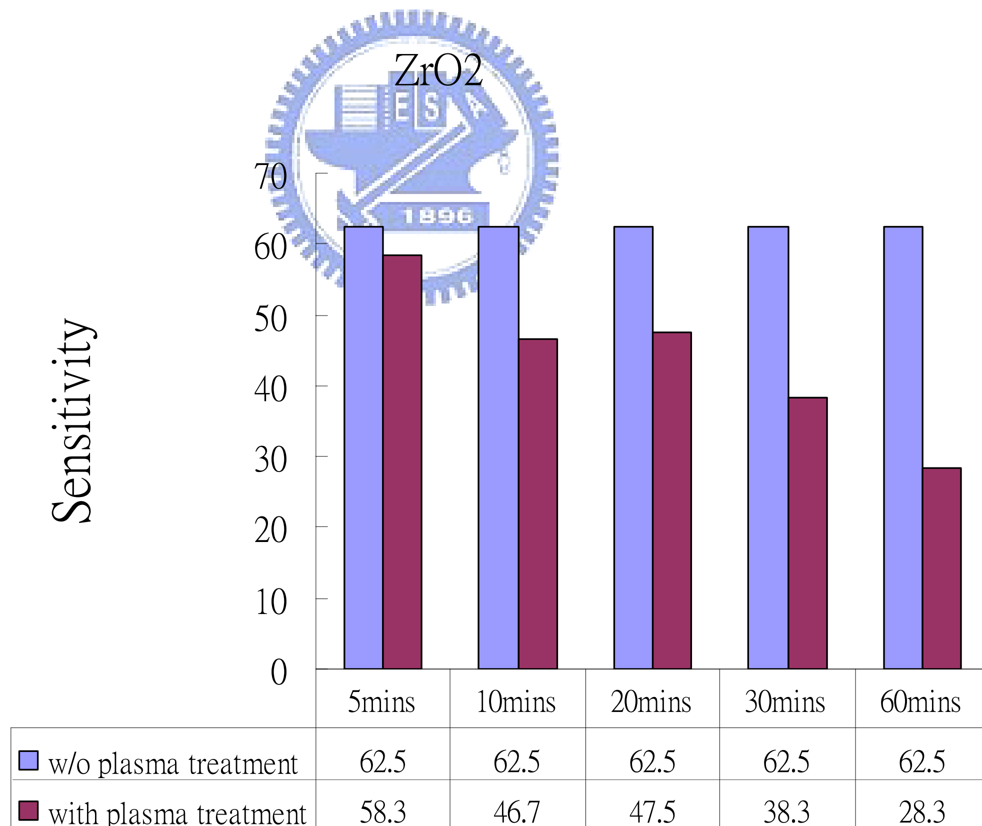

	5mins	10mins	20mins	30mins	60mins
w/o plasma treatment	62.5	62.5	62.5	62.5	62.5
with plasma treatment	58.3	46.7	47.5	38.3	28.3

Fig 4.26 The tendency of various plasma treating time intervals of ZrO_2

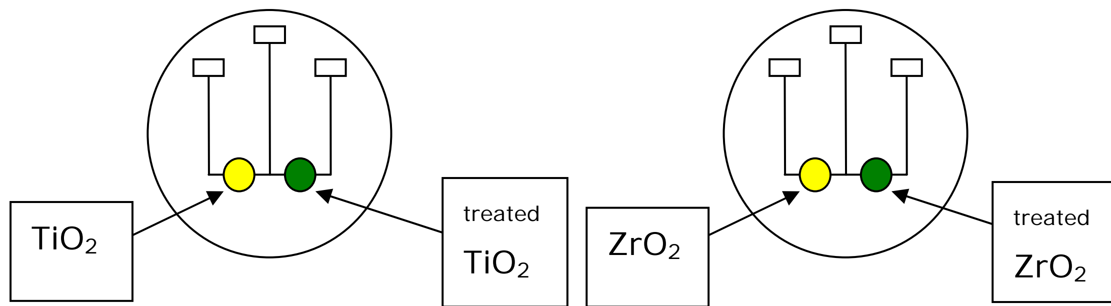

Fig 4.27 The coplanar structure